Table 1: Viral infections in humans associated with autoimmune diseases.

Relevance or suspicion of autoimmune human diseases	Representative viruses
PBC	HIV-1 p24
	MMTV
Multiple sclerosis	Epstein-Barr virus (EBV) Measles virus
Type1 diabetes	Coxsackie virus B4
	Rubella virus
	Cytomegalovirus (CMV) Mumps virus
Rheumatoid arthritis	EBV
	Hepatitis C virus (HCV)
Systemic lupus erythematosus	EBV
Myocarditis	Coxsackievirus B3
	CMV
Myasthenia gravis	Herpes simplex virus
	HCV
Guillain-Barre syndrome	CMV
	EBV

PBC because of the tendency of several viruses to target particularly the liver. There are several mechanisms by which viruses are thought to induce an autoimmune response. These include the expression of some autoantigens, the expression of major histocompatibility complex molecules, and changes in cytokine production [16]. To understand the etiology of PBC associated with infection, several factors should be considered and especially animal models may be useful [14, 17]. The association of betaretroviral protein production and aberrant PDC-E2-like protein expression in the IL-2R$\alpha^{-/-}$ mouse and Nonobese diabetic (NOD).c3c4 mouse was reported recently [18].

In this paper, we introduce three typical animal models of PBC: the dominant-negative form of transforming growth factor-β receptor type II (dnTGFβRII) mouse, IL-2R$\alpha^{-/-}$ mouse, and NOD.c3c4 mouse are enumerated and described [19–21]. Additionally, we discuss previous reports of viral infection associated with PBC and consider the etiology of PBC from our analysis of results in NOD.c3c4 mouse.

2. Murine Model of PBC

2.1. DnTGFβRII Mouse. TGF-β is the most widely distributed cytokine with pleiotropic effects on cell growth and immunological controls, specifically having a promoting effect on the development of the regulatory T-cell compartment [22]. dnTGFβRII mice were originally developed by Gorelik and Flavell for the purpose of analyzing the role of this receptor, which regulates the activation of the T cell function [23]. To disrupt the intracellular domain of the normal receptor in this mouse, the receptor is incompetent of transduction after TGF-β ligation. The expression of dnTGFβRII is limited by the CD4 promotor which lacks CD8 silencer, and this transgenic mouse spontaneously develops features characteristic of PBC [23]. These features include the expression of AMA with specificity against PDC-E2, BCOADC-E2, and OGDC-E2, as in human PBC. Pathologically, the infiltration of lymphoid cells, especially $CD4^+$ and $CD8^+$ lymphocytes, in the portal tracts causes biliary duct destruction [19] and the accumulation of natural killer T cells (NKT) in the intrahepatic bile duct lesions, resembling the condition found in human PBC [24]. Although the granuloma formations around the portal tracts seen in human PBC are not present, some lymphocytic aggregations like immature granuloma formation could be observed [25]. Furthermore, the serum levels of cytokines such as IFN-γ,TNF-α,IL-12p40, and IL-6 are significantly increased, as seen in human PBC [26, 27].

2.2. IL-2R$\alpha^{-/-}$ Mouse. In 2006, Aoki et al. reported a male child with a genetic deficiency of IL-2 receptor αIL-2Rα,)CD25) expression who had liver dysfunction with serological expression of PBC. Histologically, there was lymphoid infiltration in the portal tracts and serum antibody to PDC-E2. The deficiency of $CD4^+$ $CD25^+$ subset of regulatory T cells was considered a key to elucidating of this clinical condition [20]. Based on these findings, Wakabayashi et al. established IL-2R$\alpha^{-/-}$ mice and evaluated their hepatic immunopathology [28]. These mice also show AMA positivity against PDC-E2 that localizes to the inner lipoyl domain of the autoantigen. Lymphoid cells, composed of $CD4^+$ and $CD8^+$ lymphocytes, infiltrate into portal tracts without a significant increase in NKT. Although mild interface hepatitis and biliary duct destruction are seen in the liver, granuloma formations around the portal tracts are not observed [28]. The circulating cytokine profiles are similar to those of dnTGFβRII mice, showing elevations of IFN-γ,TNF-α,IL-12p40, and IL-6, as identified in the serum of patients with PBC [26, 27, 29].

2.3. NOD.c3c4 Mouse. NOD.c3c4 mice were generated by the introgression of large genetic intervals on chromosome 3 and 4 into a NOD background [21, 30]. NOD and genetically modified NOD mice have been reported to progress to not only spontaneous autoimmune diabetes but also rheumatoid arthritis, Sjogren's syndrome, and thyroiditis [31–34]. NOD.c3c4 mice derived from NOD strains are considered to be an animal model of PBC with autoimmune biliary destruction [21, 30]. Most importantly, these mice show antibodies to PDC-E2. They express AMA positivity, unlike the dnTGFβRII mice and IL-2R$\alpha^{-/-}$ mice, and the rate of positivity has reached 50–60% [35]. Portal tract infiltration with $CD3^+$, $CD4^+$, and $CD8^+$ lymphocytes results in chronic nonsuppurative destructive cholangitis and epithelioid granuloma formations [21, 30]. However, the morphological features of the bile ducts lesions differ from those in human PBC, in which characteristic biliary cyst formations as well as apparent hepatomegaly are described [36].

Table 2: Antiviral trials for PBC.

Trial	Method	Subject	Design	Primary outcome	Year	Reference
Pilot studies of single and combination antiretroviral therapy	Lamivudine + Zidovudine versus Lamivudine	Human	Randomized controlled trial (RCT)	Serological improvements of alkaline phos-phatase, AST and ALT. Histological improvement in necroinflammatory score and a reduction in bile duct injury.	2004	[43]
Clinical trial: randomized controlled trial of lamivudine and zidovudine (Combivir)	Lamivudine + Zidovudine + UDCA versus UDCA	Human	RCT	Serological improvements in serial alkaline phosphatase, ALT and AST.	2008	[44]
Randomized controlled trial of lamivudine	Lamivudine versus UDCA	Human	RCT	One case showed a decrease of AMA titers.	2010	[45]
Combination antiretroviral therapy with Combivir	Lamivudine + Zidovudine versus Placebo	NOD.c3c4 mouse		Histological improvement in necroinflammatory score and a reduction in bile duct injury. No improvement on bile duct cyst. Decrease in viral burden.	2007	[46]
Highly active antiretroviral therapy with reverse transcriptase inhibitors and protease inhibitor	Combination of reverse transcriptase and protease inhibitor	NOD.c3c4 mouse		Serological improvements in alkaline phos-phatase and AST. Complete disappearance of cholangitis.	2008	[47]

3. Possibility of Viral Infection Associated with PBC

It has been thought that some viruses may associate with human diseases of oncogenesis or autoimmunity because of their genome integration or specific viral-encoding proteins. Especially, in 1998, Munoz et al. described that there was an antibody for human immunodeficiency virus-1 (HIV-1) in the serum of PBC patients [37]. To investigate for a possible immune response to the p24 gag protein of HIV-1, moderate-to-strong reactivity was found in about 30% of the patients with Sjogren's syndrome, as compared with less than 1% of healthy controls [38], and the 36% of systemic lupus erythematosus (SLE) patients produced antibodies to the p24 gag protein [39]. Mason et al. discovered HIV-1 p24 gag protein seroreactivity in 35% of patients with PBC, 29% of patients with SLE, and 39% of patients with either primary sclerosing cholangitis or biliary atresia, compared with only 4% of patients with alcohol-related liver disease or alpha1-antitrypsin-deficiency liver disease, and only 4% of healthy volunteers. Moreover, Western blot reactivity to the human intracisternal A-type particle (HIAP) proteins related to HIV-1 was found in 51% of patients with PBC, in 58% patients with SLE, and in 17% of those with other biliary diseases. None of the 23 patients with either alcohol-related liver disease or alpha1-antitrypsin deficiency and only one of the healthy controls showed the same reactivity to HIAP proteins [40]. Therefore, these antibody reactivities found in patients with PBC may be attributable to an immune response to uncharacterized viral proteins that share antigenic determinants with HIV-1-related retroviruses.

In 2003, a human betaretrovirus clone sequence was originally detected from the biliary epithelium cDNA library of a patient with PBC. When searching viral data registered in BLASTN, the initial partial pol gene fragment was found to exhibit 95% to 97% identities with mouse mammary tumor virus (MMTV) and with retrovirus sequences derived from human breast cancer samples within the overlapping sequence [12, 41]. Using a specific MMTV antibody, viral proteins were shown in the perihepatic lymph nodes but not in liver tissue samples from patients with PBC [41]. However, Selmi et al. expressed an opposing view concerning this result [42].

Some pilot studies were conducted to determine whether antiviral therapy impacted the disease progression (Table 2). First, Mason et al. performed a trial with reverse-transcriptase inhibitors (lamivudine group versus lamivudine/zidovudine group) for patients with PBC. The lamivudine/zidovudine group showed significant serological improvement in the activities of alkaline phosphatase, AST and ALT, and histological assessment revealed an improvement in the necroinflammatory score and a reduction in bile duct injury compared to the lamivudine group [43]. A further clinical trial was performed with a combination of lamivudine and zidovudine versus ursodeoxycholic acid (UDCA). Significant differences were observed in the antiviral therapy versus UDCA with serological improvements in serial alkaline phosphatase, ALT and AST as well as the clinical score [44]. Thus, reverse-transcriptase inhibitors are

expected to suppress retroviral proliferation and contribute to the improvement of PBC. We once investigated the efficacies of 90 day's administration of lamivudine to 20 PBC patients with unsatisfactory biochemical responses to UDCA in a randomized double blind control trial. As a result, no significant biochemical difference was seen between both groups. However, of interest, one case showed a decrease of AMA titers and biochemical response [45]. These results were similar to those of studies conducted by Mason et al. [43]; yet the true efficacy should be evaluated in large-scale control trials.

4. Are NOD.c3c4 Mice Infected with a Retrovirus?

NOD.c3c4 mice have been described as a mouse model with several features similar to PBC [30]. However, these mice develop marked biliary cyst formation that is not shown in human PBC. In human PBC, the destruction of cholangiocytes leads to ductpenia [48]. When we analyzed the gene expression of the cholangiocytes of such mice using microarray analysis, there was consistent liver-specific downregulation in the expression of Fas antigen (CD95) [36]. Fas (CD95) antigen is a member of the tumor necrosis factor family that binds to Fas ligand (FasL). This gene is situated at chromosome 19 in mouse [49]. Fas/FasL interactions play an important role in apoptosis [49–51]. Fas is detected in hepatocytes and plays an important role in inflammation and cell death in hepatitis virus-infected liver [52]. The Fas system on cholangiocytes has been also reported in human and rats, and enhanced expression of FasL on cholangiocytes has been implicated in progressive bile duct loss in PBC through apoptosis [53]. Furthermore, FasL expressed by cholangiocarcinomas was reported to induce lymphocyte cell death and escape immune surveillance [54]. It has been reported that the Fas/FasL system is strongly associated with biliary pathological conditions. It was thought that, because of the downregulation of Fas antigen, the apoptosis of cholangiocytes cannot easily occur and therefore biliary cyst formation was found in NOD.c3c4 mice [36]. However, it was considered that there are also other factors because the degree of the cyst formation differed according to the individual though the genetic expression was the same.

In 2007, Chen et al. reported that MMTV gag and pol gene expression was 4- to 25-fold higher in all three autoimmune biliary disease models, NOD.c3c4, dnTGF-βRII, and IL-2R$\alpha^{-/-}$, as compared to control mice when using real-time RT-PCR to quantify MMTV using gag and pol primers [55]. A randomized study was conducted using NOD.c3c4 mice treated with a combination therapy of lamivudine and zidovudine or with placebo (Table 2). Serial hepatic biochemistry studies showed diminished alkaline phosphatase in the mice treated with combination therapy. Histological evaluation showed a significant decrease in the necroinflammatory score and the grade of the bile duct injury in the combination therapy group. However, therapy had little improvement on bile duct cyst formation. When compared to mice receiving placebo group, combination therapy group reduced viral burden measured by the pol and gag gene RT-PCR [46]. Moreover, Graham et al. treated NOD.c3c4 mice with combination of reverse transcriptase inhibitors and protease inhibitor. Hepatic biochemistry showed significant improvements in alkaline phosphatase and AST, and the cholangitis completely disappeared [47]. Thus, the detection of MMTV in the NOD.c3c4 mice and resolution of biliary disease with antiviral therapy supports the retroviral hypothesis for PBC.

However, in order to prove that viral factors are involved in the pathogenesis of PBC, it is necessary to understand and elucidate the mechanism of viral replication, reproduction, the transcription of the virus genomes, the pathogenic roles of viral tropics, the integrated state, and the interaction with the host's immune system, especially the mechanism by which autoimmune tolerance is broken. Therefore, it is premature to relate the cause of the clinical condition of PBC to viral infection based only on the present report. However, given the unprecedented progress of biotechnology, a more detailed understanding of these issues can be expected in the near future.

References

[1] Y. Nakanuma and G. Ohta, "Histometric and serial section observations of the intrahepatic bile ducts in primary biliary cirrhosis," *Gastroenterology*, vol. 76, no. 6, pp. 1326–1332, 1979.

[2] M. E. Gershwin, I. R. Mackay, A. Sturgess, and R. L. Coppel, "Identification and specificity of a cDNA encoding the 70 KD mitochondrial antigen recognized in primary biliary cirrhosis," *Journal of Immunology*, vol. 138, no. 10, pp. 3525–3531, 1987.

[3] R. L. Coppel, L. J. McNeilage, C. D. Surh et al., "Primary structure of the human M2 mitochondrial autoantigen of primary biliary cirrhosis: dihydrolipoamide acetyltransferase," *Proceedings of the National Academy of Sciences of the United States of America*, vol. 85, no. 19, pp. 7317–7321, 1988.

[4] J. van de Water, A. A. Ansari, C. D. Surh et al., "Evidence for the targeting by 2-oxo-dehydrogenase enzymes in the T cell response of primary biliary cirrhosis," *Journal of Immunology*, vol. 146, no. 1, pp. 89–94, 1991.

[5] D. E. J. Jones, J. M. Palmer, O. F. W. James, S. J. Yeaman, M. F. Bassendine, and A. G. Diamond, "T-cell responses to the components of pyruvate dehydrogenase complex in primary biliary cirrhosis," *Hepatology*, vol. 21, no. 4, pp. 995–1002, 1995.

[6] K. Harada, S. Ozaki, M. E. Gershwin, and Y. Nakanuma, "Enhanced apoptosis relates to bile duct loss in primary biliary cirrhosis," *Hepatology*, vol. 26, no. 6, pp. 1399–1405, 1997.

[7] J. A. Odin, R. C. Huebert, L. Casciola-Rosen, N. F. LaRusso, and A. Rosen, "Bcl-2-dependent oxidation of pyruvate dehydrogenase-E2, a primary biliary cirrhosis autoantigen, during apoptosis," *Journal of Clinical Investigation*, vol. 108, no. 2, pp. 223–232, 2001.

[8] A. Tanaka, P. S. C. Leung, T. P. Kenny et al., "Genomic analysis of differentially expressed genes in liver and biliary epithelial cells of patients with primary biliary cirrhosis," *Journal of Autoimmunity*, vol. 17, no. 1, pp. 89–98, 2001.

[9] S. P. M. Fussey, S. T. Ali, J. R. Guest, O. F. W. James, M. F. Bassendine, and S. J. Yeaman, "Reactivity of primary biliary

cirrhosis sera Escherichia coli dihydrolipoamide acetyltransferase (E2p): characterization of the main immunogenic region," *Proceedings of the National Academy of Sciences of the United States of America*, vol. 87, no. 10, pp. 3987–3991, 1990.

[10] S. A. Long, C. Quan, J. van de Water et al., "Immunoreactivity of organic mimeotopes of the E2 component of pyruvate dehydrogenase: connecting xenobiotics with primary biliary cirrhosis," *Journal of Immunology*, vol. 167, no. 5, pp. 2956–2963, 2001.

[11] P. S. C. Leung, C. Quan, O. Park et al., "Immunization with a xenobiotic 6-bromohexanoate bovine serum albumin conjugate induces antimitochondrial antibodies," *Journal of Immunology*, vol. 170, no. 10, pp. 5326–5332, 2003.

[12] L. Xu, Z. Shen, L. Guo et al., "Does a betaretrovirus infection trigger primary biliary cirrhosis?" *Proceedings of the National Academy of Sciences of the United States of America*, vol. 100, no. 14, pp. 8454–8459, 2003.

[13] G. Schembri and P. Schober, "Killing two birds with one stone," *The Lancet*, vol. 377, no. 9759, p. 96, 2011.

[14] N. R. Rose, "Mechanisms of autoimmunity," *Seminars in Liver Disease*, vol. 22, no. 4, pp. 387–394, 2002.

[15] S. Shimoda, M. Nakamura, H. Ishibashi, K. Hayashida, and Y. Niho, "HLA DRB4 0101-restricted immunodominant T cell autoepitope of pyruvate dehydrogenase complex in primary biliary cirrhosis: evidence of molecular mimicry in human autoimmune diseases," *Journal of Experimental Medicine*, vol. 181, no. 5, pp. 1835–1845, 1995.

[16] J. van de Water, H. Ishibashi, R. L. Coppel, and M. E. Gershwin, "Molecular mimicry and primary biliary cirrhosis: premises not promises," *Hepatology*, vol. 33, no. 4, pp. 771–775, 2001.

[17] M. Regner and P. H. Lambert, "Autoimmunity through infection or immunization?" *Nature immunology*, vol. 2, no. 3, pp. 185–188, 2001.

[18] G. Zhang, M. Chen, D. Graham et al., "Mouse mammary tumor virus in anti-mitochondrial antibody producing mouse models," *Journal of Hepatology*. In press.

[19] S. Oertelt, Z. X. Lian, C. M. Cheng et al., "Anti-mitochondrial antibodies and primary biliary cirrhosis in TGF-β receptor II dominant-negative mice," *Journal of Immunology*, vol. 177, no. 3, pp. 1655–1660, 2006.

[20] C. A. Aoki, C. M. Roifman, Z. X. Lian et al., "IL-2 receptor alpha deficiency and features of primary biliary cirrhosis," *Journal of Autoimmunity*, vol. 27, no. 1, pp. 50–53, 2006.

[21] S. Koarada, Y. Wu, N. Fertig et al., "Genetic control of autoimmunity: protection from diabetes, but spontaneous autoimmune biliary disease in a nonobese diabetic congenic strain," *Journal of Immunology*, vol. 173, no. 4, pp. 2315–2323, 2004.

[22] J. Massague, "TGF-beta signal transduction," *Annual Review of Biochemistry*, vol. 67, pp. 753–791, 1998.

[23] L. Gorelik and R. A. Flavell, "Abrogation of TGFβ signaling in T cells leads to spontaneous T cell differentiation and autoimmune disease," *Immunity*, vol. 12, no. 2, pp. 171–181, 2000.

[24] K. Harada, K. Isse, K. Tsuneyama, H. Ohta, and Y. Nakanuma, "Accumulating $CD57^+CD3^+$ natural killer T cells are related to intrahepatic bile duct lesions in primary biliary cirrhosis," *Liver International*, vol. 23, no. 2, pp. 94–100, 2003.

[25] S. Oertelt, W. M. Ridgway, A. A. Ansari, R. L. Coppel, and M. E. Gershwin, "Murine models of primary biliary cirrhosis: comparisons and contrasts," *Hepatology Research*, vol. 37, no. 3, pp. S365–S369, 2007.

[26] M. Shindo, G. E. Mullin, L. Braun-Elwert, N. V. Bergasa, E. A. Jones, and S. P. James, "Cytokine mRNA expression in the liver of patients with primary biliary cirrhosis (PBC) and chronic hepatitis B (CHB)," *Clinical and Experimental Immunology*, vol. 105, no. 2, pp. 254–259, 1996.

[27] M. Yasoshima, N. Kono, H. Sugawara, K. Katayanagi, K. Harada, and Y. Nakanuma, "Increased expression of inter-leukin-6 and tumor necrosis factor-α in pathologic biliary epithelial cells: in situ and culture study," *Laboratory Investigation*, vol. 78, no. 1, pp. 89–100, 1998.

[28] K. Wakabayashi, Z. X. Lian, Y. Moritoki et al., "IL-2 receptor $\alpha^{-/-}$ mice and the development of primary biliary cirrhosis," *Hepatology*, vol. 44, no. 5, pp. 1240–1249, 2006.

[29] P. A. Berg, R. Klein, and M. Röcken, "Cytokines in primary biliary cirrhosis," *Seminars in Liver Disease*, vol. 17, no. 2, pp. 115–123, 1997.

[30] J. Irie, Y. Wu, L. S. Wicker et al., "NOD.c3c4 congenic mice develop autoimmune biliary disease that serologically and pathogenetically models human primary biliary cirrhosis," *Journal of Experimental Medicine*, vol. 203, no. 5, pp. 1209–1219, 2006.

[31] P. Humbert and J. L. Dupond, "Multiple autoimmune syndromes (MAS)," *Annales de Medecine Interne*, vol. 139, no. 3, pp. 159–168, 1988.

[32] K. O. Gtc, C. C. Szeto, V. Yeung, C. C. Chow, H. Chan, and C. S. Cockram, "Autoimmune polyglandular syndrome and primary biliary cirrhosis," *British Journal of Clinical Practice*, vol. 50, no. 6, pp. 344–346, 1996.

[33] J. P. Lin, J. M. Cash, S. Z. Doyle et al., "Familial clustering of rheumatoid arthritis with other autoimmune diseases," *Human Genetics*, vol. 103, no. 4, pp. 475–482, 1998.

[34] M. M. Griffiths, J. A. Encinas, E. F. Remmers, V. K. Kuchroo, and R. L. Wilder, "Mapping autoimmunity genes," *Current Opinion in Immunology*, vol. 11, no. 6, pp. 689–700, 1999.

[35] Y. Ueno, Y. Moritoki, T. Shimosegawa, and M. E. Gershwin, "Primary biliary cirrhosis: what we know and what we want to know about human PBC and spontaneous PBC mouse models," *Journal of Gastroenterology*, vol. 42, no. 3, pp. 189–195, 2007.

[36] Y. Nakagome, Y. Ueno, T. Kogure et al., "Autoimmune cholangitis in NOD.c3c4 mice is associated with cholangiocyte-specific Fas antigen deficiency," *Journal of Autoimmunity*, vol. 29, no. 1, pp. 20–29, 2007.

[37] S. Munoz, S. Ballas, R. Norberg, and W. Maddrey, "Antibodies to human immunodeficiency virus (HIV) in primary biliary cirrhosis," *Gastroenterology*, vol. 94, p. A574, 1988.

[38] N. Talal, M. J. Dauphinee, H. Dang, S. S. Alexander, D. J. Hart, and R. F. Garry, "Detection of serum antibodies to retroviral proteins in patients with primary Sjogren's syndrome (autoimmune exocrinopathy)," *Arthritis and Rheumatism*, vol. 33, no. 6, pp. 774–781, 1990.

[39] N. Talal, R. F. Garry, P. H. Schur et al., "A conserved idiotype and antibodies to retroviral proteins in systemic lupus erythematosus," *Journal of Clinical Investigation*, vol. 85, no. 6, pp. 1866–1871, 1990.

[40] A. L. Mason, L. Xu, L. Guo et al., "Detection of retroviral antibodies in primary biliary cirrhosis and other idiopathic biliary disorders," *The Lancet*, vol. 351, no. 9116, pp. 1620–1624, 1998.

[41] L. Xu, M. Sakalian, Z. Shen, G. Loss, J. Neuberger, and A. Mason, "Cloning the human betaretrovirus proviral genome from patients with primary biliary cirrhosis," *Hepatology*, vol. 39, no. 1, pp. 151–156, 2004.

[42] C. Selmi, S. R. Ross, A. A. Ansari et al., "Lack of immunological or molecular evidence for a role of mouse mammary tumor

retrovirus in primary biliary cirrhosis," *Gastroenterology*, vol. 127, no. 2, pp. 493–501, 2004.

[43] A. L. Mason, G. H. Farr, L. Xu, S. G. Hubscher, and J. M. Neuberger, "Pilot studies of single and combination antiretroviral therapy in patients with primary biliary cirrhosis," *American Journal of Gastroenterology*, vol. 99, no. 12, pp. 2348–2355, 2004.

[44] A. L. Mason, K. D. Lindor, B. R. Bacon, C. Vincent, J. M. Neuberger, and S. T. Wasilenko, "Clinical trial: randomized controlled study of zidovudine and lamivudine for patients with primary biliary cirrhosis stabilized on ursodiol," *Alimentary Pharmacology and Therapeutics*, vol. 28, no. 7, pp. 886–894, 2008.

[45] K. Fukushima, Y. Ueno, and T. Shimosegawa, "Treatment of primary biliary cirrhosis: a new challenge?" *Hepatology Research*, vol. 40, no. 1, pp. 61–68, 2010.

[46] M. Chen, D. Graham, S. Girgis et al., "Combination antiretroviral therapy with Combivir attenuates autoimmune biliary disease in the NOD.c3c4 mouse model of primary biliary cirrhosis," *Hepatology*, vol. 46, supplement 1, p. 548A, 2007.

[47] D. Graham, M. Chen, S. Girgis, G. Zhang, and A. Mason, "Highly active anti-retroviral therapy completely abrogates cholangitis in the NOD.c3c4 mouse model of PBC," *Journal of Hepatology*, vol. 2, p. s54, 2008.

[48] G. R. Locke III, T. M. Therneau, J. Ludwig, E. R. Dickson, and K. D. Lindor, "Time course of histological progression in primary biliary cirrhosis," *Hepatology*, vol. 23, no. 1, pp. 52–56, 1996.

[49] S. Nagata and P. Golstein, "The Fas death factor," *Science*, vol. 267, no. 5203, pp. 1449–1456, 1995.

[50] T. Sakai, Y. Kimura, K. Inagaki-Ohara, K. Kusugami, D. H. Lynch, and Y. Yoshikai, "Fas-mediated cytotoxicity by intestinal intraepithelial lymphocytes during acute graft-versus-host disease in mice," *Gastroenterology*, vol. 113, no. 1, pp. 168–174, 1997.

[51] Y. Ueno, M. Ishii, K. Yahagi et al., "Fas-mediated cholangiopathy in the murine model of graft versus host disease," *Hepatology*, vol. 31, no. 4, pp. 966–974, 2000.

[52] N. Hiramatsu, N. Hayashi, K. Katayama et al., "Immunohistochemical detection of Fas antigen in liver tissue of patients with chronic hepatitis C," *Hepatology*, vol. 19, no. 6, pp. 1354–1359, 1994.

[53] M. Iwata, K. Harada, K. Hiramatsu et al., "Fas ligand expressing mononuclear cells around intrahepatic bile ducts co-express CD68 in primary biliary cirrhosis," *Liver*, vol. 20, no. 2, pp. 129–135, 2000.

[54] F. G. Que, V. A. Phan, V. H. Phan et al., "Cholangiocarcinomas express Fas ligand and disable the Fas receptor," *Hepatology*, vol. 30, no. 6, pp. 1398–1404, 1999.

[55] M. Chen, D. Graham, G. Zhang et al., "Biliary infection with mouse mammary tumor virus in the NOD.c3c4 mouse and other mouse models of primary biliary cirrhosis," *Hepatology*, vol. 46, supplement 1, p. 551A, 2007.

JCM
Journals.ASM.org

Use of Illumina Deep Sequencing Technology To Differentiate Hepatitis C Virus Variants

Masashi Ninomiya,[a] Yoshiyuki Ueno,[a] Ryo Funayama,[b] Takeshi Nagashima,[b] Yuichiro Nishida,[b] Yasuteru Kondo,[a] Jun Inoue,[a] Eiji Kakazu,[a] Osamu Kimura,[a] Keiko Nakayama,[b] and Tooru Shimosegawa[a]

Division of Gastroenterology, Tohoku University of Medicine, Sendai, Japan,[a] and Division of Cell Proliferation, Tohoku University of Medicine, Sendai, Japan[b]

Hepatitis C virus (HCV) is a positive-strand enveloped RNA virus that shows diverse viral populations even in one individual. Though Sanger sequencing has been used to determine viral sequences, deep sequencing technologies are much faster and can perform large-scale sequencing. We demonstrate the successful use of Illumina deep sequencing technology and subsequent analyses to determine the genetic variants and amino acid substitutions in both treatment-naïve (patient 1) and treatment-experienced (patient 7) isolates from HCV-infected patients. As a result, almost the full nucleotide sequence of HCV was detectable for patients 1 and 7. The reads were mapped to the HCV reference sequence. The coverage was 99.8% and the average depth was 69.5× for patient 7, with values of 99.4% (coverage) and 51.1× (average depth) for patient 1. In patient 7, amino acid (aa) 70 in the core region showed arginine, with methionine at aa 91, by Sanger sequencing. Major variants showed the same amino acid sequence, but minor variants were detectable in 18% (6/34 sequences) of sequences, with replacement of methionine by leucine at aa 91. In NS3, 8 amino acid positions showed mixed variants (T72T/I, K213K/R, G237G/S, P264P/S/A, S297S/A, A358A/T, S457S/C, and I615I/M) in patient 7. In patient 1, 3 amino acid positions showed mixed variants (L14L/F/V, S61S/A, and I586T/I). In conclusion, deep sequencing technologies are powerful tools for obtaining more profound insight into the dynamics of variants in the HCV quasispecies in human serum.

Hepatitis C virus (HCV) is a positive-strand enveloped RNA virus of approximately 9,600 nucleotide (nt) bases, consisting of a single open reading frame and two untranslated regions, and belongs to the genus *Hepacivirus* within the family *Flaviviridae* (6). The single open reading frame encodes a polyprotein of 3,011 amino acids (aa) that is cleaved by viral and cellular proteases into 10 different proteins. The three structural proteins, which constitute the viral particle, include the core protein and the envelope glycoproteins E1 and E2. Two regions in E2, known as hypervariable regions 1 and 2, are reported to have extreme sequence variability. The seven nonstructural components include the p7 polypeptide, the NS2-3 protease, the NS3 serine protease and RNA helicase, the NS4A polypeptide, the NA4B and NS5A proteins, and the NS5B RNA-dependent RNA polymerase (RdRp) (29). At both ends of the open reading frame lie the 5′- and 3′-untranslated regions (5′-UTR and 3′-UTR). The nucleotide sequence of the 5′-UTR is relatively well conserved among different HCV genotypes. The HCV 5′-UTR contains an internal ribosome entry site (IRES) that directs the cap-independent initiation of virus translation and forms on four characteristic stem-loop structures (17, 18). HCV displays very high genetic variability both in populations and within infected individuals, where it exists as a cluster of closely related but distinct variants, termed "quasispecies," as occurs in many other RNA viruses with a polymerase enzyme lacking proofreading ability (6, 8, 26).

Current standard treatment of chronic HCV infection is based on the combination of pegylated alpha interferon (peg-IFN-α) and ribavirin (RBV). However, patients with a high load of genotype 1b virus ($>1 \times 10^5$ log IU/ml) do not achieve high sustained virological response (SVR) rates (<50%), even when the most effective combination treatment (IFN plus RBV) is administered for 48 weeks (14, 25). Some investigations concerning therapeutic prediction based on virological features revealed that substitutions of arginine for glutamine at amino acid (aa) 70 and/or leucine for methionine at aa 91 in the core region are independent and significant factors associated with SVR or that patients whose viruses have more than 4 amino acid changes in the NS5A interferon sensitivity-determining region (ISDR) (aa 2209 to 2248) have high responses to IFN therapy compared to those for patients with HCV-J (mutant type), whereas patients whose viruses have no amino acid changes (wild type) or 1 to 3 amino acid changes (intermediate type) have low responses (1, 2, 9, 10).

Recently, direct-acting antiviral (DAA) molecules active on HCV, such as NS3/4A protease inhibitors, nucleoside/nucleotide analogue inhibitors of RdRp, nonnucleoside inhibitors of RdRp, and NS5A inhibitors, have been developed. These DAA molecules, either alone or in combination with peg-IFN plus RBV, were recently described as showing large antiviral effects (15, 21). However, the problem that we have to consider next is viral resistance to DAAs due to the selection of viral variants that contain amino acid substitutions altering the drug target and rendering virus less susceptible to the drug's inhibitory activity (35). Additionally, drug-resistant variants already preexist as minor populations within a patient's quasispecies. Drug exposure intensively inhibits replication of the drug-sensitive viral population, and the resistant variants gradually predominate in the HCV population (7). In the future, to determine the most appropriate treatment for HCV

Received 7 September 2011 Returned for modification 10 October 2011
Accepted 9 December 2011
Published ahead of print 28 December 2011
Address correspondence to Yoshiyuki Ueno, yueno@med.tohoku.ac.jp.
Supplemental material for this article may be found at http://jcm.asm.org/.

doi:10.1128/JCM.05715-11

patients, analysis of the nucleotide or amino acid sequence of HCV will become important.

Initial attempts to identify the HCV genome sequence relied on Sanger sequencing and the use of PCR primers targeting relatively conserved regions, methods that would likely fail if the virus had more variants (32–34). In recent years, new technologies have been developed that are able to sequence viruses from environmental samples without using specific primers, cloning, and resorting by recombinant DNA techniques and thus can obtain the sequence information for the complete virome in an unbiased way. Metagenomic approaches such as deep sequencing have proven increasingly successful at identifying variants or mutations of the nucleotide sequence (23, 42, 45).

Here we demonstrate the successful use of Illumina deep sequencing technology and subsequent analyses to determine the genetic variants and amino acid substitutions of both treatment-naïve (patient 1) and treatment-experienced (IFN) (patient 7) isolates of HCV without using specific HCV primers.

MATERIALS AND METHODS

Patients. Two patients with chronic hepatitis C virus infection with genotype 1b virus and one healthy control were enrolled in this study. Each serum sample was collected before treatment with peg-IFN-α and RBV and was stored at −20°C until testing. In the laboratory data, the HCV load was 6.8 log IU/ml for patient 1, who was treatment naïve, and 7.0 log IU/ml for patient 7, who was treated with IFN-α2b and RBV for 6 months in 2002, but with no treatment effect (Cobas TaqMan HCV test; Roche Molecular Systems, Pleasanton, CA). More clinical information is described in Table 1.

Sanger sequencing in the core region and NS5A ISDR. Total RNA was extracted from 100-μl serum samples by use of a MagMAX viral RNA isolation kit (Ambion, Austin, TX), and the RNA preparation thus obtained was subjected to cDNA synthesis with reverse transcriptase (SuperScript III RNase H$^-$ reverse transcriptase; Invitrogen) and to PCR amplification using Prime Star HS DNA polymerase (TaKaRa Bio, Shiga, Japan) with nested primers derived from the core region and the NS5A ISDR of the HCV genome. Nested PCR amplification of the core region of the HCV genome was carried out with primers C008 (sense; 5′-AAC CTC AAA GAA AAA CCA AAC G-3′) and C011 (antisense; 5′-CAT GGG GTA CAT YCC GCT YG-3′) in the first round, for 35 cycles (98°C for 10 s, 55°C for 15 s, and 72°C for 1 min, with an additional 7 min in the last cycle), and with primers C009 (sense; 5′-CCA CAG GAC GTY AAG TTC CC-3′) and C010 (antisense; 5′-AGG GTA TCG ATG ACC TTA CC-3′) in the second round, for 25 cycles. Nested primers derived from the NS5A ISDR of the HCV genome were designed to amplify a 188-bp product, using primers C004 (sense; 5′-ATG CCC ATG CCA GGT TCC AG-3′) and C005 (antisense; 5′-AGC TCC GCC AAG GCA GAA GA-3′) in the first round and primers C006 (sense; 5′-ACC GGA TGT GGC AGT GCT CA-3′) and C007 (antisense; 5′-GTA ATC CGG GCG TGC CCA TA-3′) in the second round. The PCR products were sequenced directly on both strands by use of a BigDye Terminator, version 3.1, cycle sequencing kit on an ABI Prism 3100 genetic analyzer (Applied Biosystems, Foster City, CA). Sequence analysis was performed using Genetyx-Mac ver. 12.2.6 (Genetyx Corp., Tokyo, Japan) and ODEN (version 1.1.1) from the DNA Data Bank of Japan (National Institute of Genetics, Mishima, Japan) (19).

Library preparation and Illumina sequencing. Total RNA was extracted from 800 μl of serum by use of a MagMAX viral RNA isolation kit (Ambion) according to the manufacturer's protocol, with the slight modification that carrier RNA was not included. A library was prepared from approximately 200 ng of total RNA by use of an mRNA-seq sample prep kit (Illumina, San Diego, CA). The quality of the library was evaluated with Bioanalyzer (Agilent, Santa Clara, CA). Before deep sequencing, we confirmed the presence of the HCV genome in the libraries by conducting quantitative PCR with StepOnePlus (Applied Biosystems), using SYBR Ex

TABLE 1 Clinical data for patients enrolled in this study[a]

Patient (storage date of sample)	Sex	Age (yr)	Diagnosis	HCV RNA load (log IU/ml)	HCV genotype	Past treatment (period)	Therapeutic effect	Core aa 70	Core aa 91	No. of aa substitutions in NS5A ISDR
1 (October 2008)	Male	43	Chronic hepatitis C	6.8	1b	None	NA	Wild type	Wild type	0
7 (May 2010)	Male	57	Chronic hepatitis C	7.0	1b	IFN-α2b plus RBV (March–September 2002)	Nontherapeutic	Wild type	Mutant	0
9 (January 2011)	Female	64	Control	NA	NA	NA	NA	NA	NA	NA

[a] Abbreviations: aa, amino acid; IFN, interferon; NA, not applicable; RBV, ribavirin. All patients were negative for hepatitis B surface antigen (HBsAg) and hepatitis B surface antibody (HBsAb).

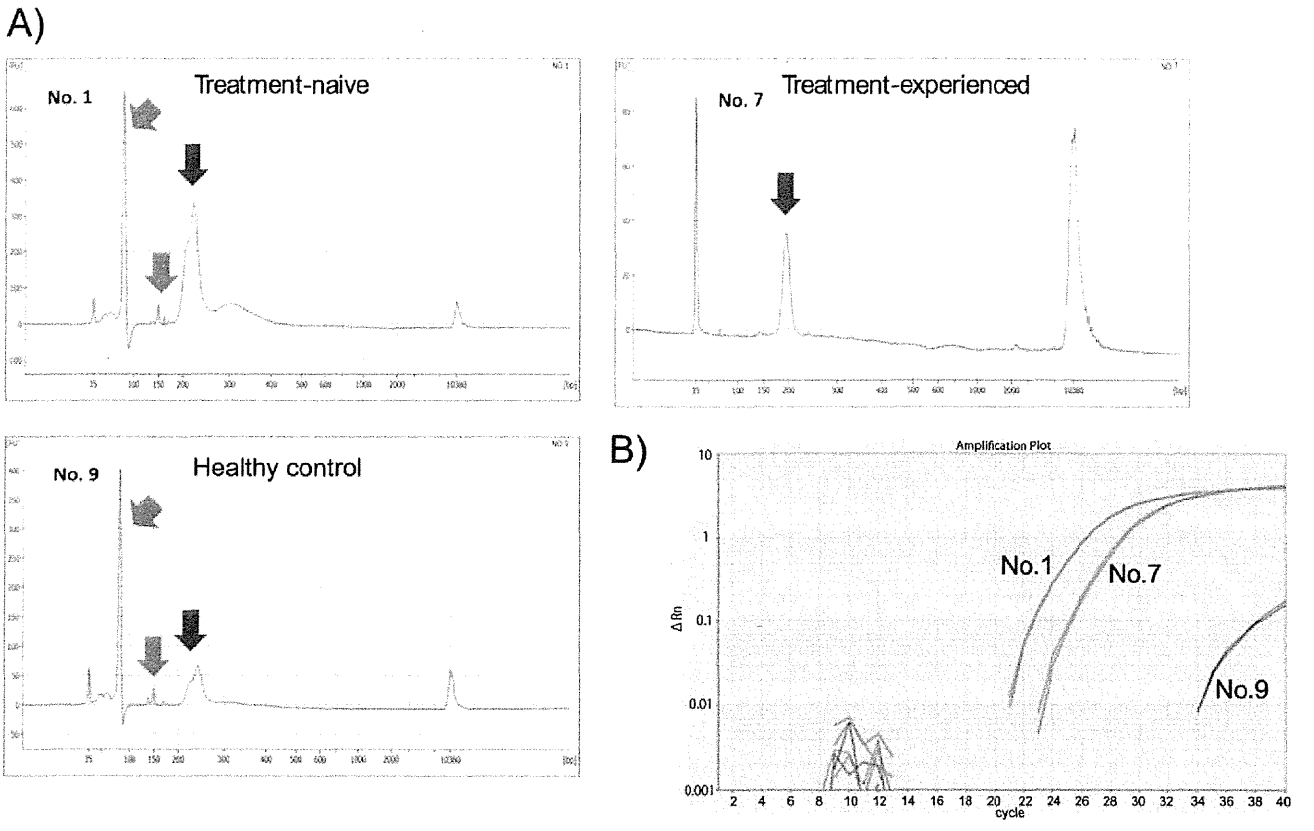

FIG 1 Evaluation of the quality of libraries. (A) The library was well refined for patient 7, but the primer and adaptor dimers were mixed in the libraries of patients 1 and 9, obtained using Bioanalyzer (Agilent). The horizontal axis shows the DNA size, and the vertical axis shows the quantity of DNA. The blue arrows indicate the desired products, and the red arrows indicate the primer or adaptor dimers. The peaks of the wave at 35 bp and 10,380 bp express the marker. (B) Amplification plots for patients 1 (treatment naïve) and 7 (treatment experienced), showing the presence of the HCV genome in the libraries by quantitative PCR with StepOnePlus (Applied Biosystems).

Taq premix (TaKaRa, Shiga, Japan) and the specific primers C112 (sense; 5′-GCW GTS CAR TGG ATG AAC CG-3′) and C113 (antisense; 5′-GCT YTC MGG CAC RTA GTG CG-3′), derived from the 81-bp region encoding HCV NS4B, and then loaded each sample into two or three lanes of a flow cell. Libraries were clonally amplified on the flow cell and sequenced on an Illumina IIx genome analyzer (SCS 2.8 software; Illumina, San Diego, CA), with a 76-mer single end sequence. Image analysis and base calling were performed using RTA 1.8 software.

Analysis. Seventy-six-mer single-end reads were classified by strict bar codes, split into individual reads, and stripped of any remaining primer sequences by using CLC Genomics Workbench (4.6) (http://www.clcbio.co.jp). Sequence reads aligned to the human genome by hg19 (http://hgdownload.cse.ucsc.edu/goldenPath/hg19/bigZips/chromFa.tar.gz), GenBank (http://hgdownload.cse.ucsc.edu/goldenPath/hg19/bigZips/mrna.fa.gz), RefSeq (http://hgdownload.cse.ucsc.edu/goldenPath/hg19/bigZips/refMrna.fa.gz), and Ensembl (ftp://ftp.ensembl.org/pub/release62/fasta/homo_sapiens/cdna/Homo_sapiens.GRCh37.62.cdna.all.fa.gz and ftp://ftp.ensembl.org/pub/release62/fasta/homo_sapiens/ncrna/Homo_sapiens.GRCh37.62.ncrna.fa.gz) were removed in the first mapping analysis of the human genome. Sequence reads not of human origin were aligned with 970 reference HCV sequences registered at the Hepatitis Virus Database server (http://s2as02.genes.nig.ac.jp/index.html) by use of BWA (0.5.9-r16), allowing mismatches within 5 to 10 nucleotide bases (24). The reads could be defined as being of HCV origin by identification with reference to the HCV sequences, allowing mismatches within 10 nucleotide bases. Duplicate reads were completely excluded to avoid sequence bias, using Samtools (0.1.16) (24). Additionally, the variants compared with HCV-J were identified by Samtools. The result of the analysis was displayed using Integrative Genomics Viewer (IGV; 2.0.3) (36).

Ethics statement. Written informed consent was obtained from each individual, and the study for detecting host genomes was approved by the Ethics Committee of the Tohoku University School of Medicine (2010-404).

RESULTS

Evaluation of the quality of the libraries. We conducted deep sequencing analysis for two patients (patient 1 [treatment naïve] and patient 7 [treatment experienced, with IFN]) who had been infected with chronic hepatitis C virus of genotype 1b, as well as one healthy control (patient 9) (Table 1). Since there is only a small quantity of circulating RNAs, including those of viral origin, in serum, it was important to evaluate the quality of the libraries. The library for patient 7 showed good quality using an Agilent bioanalyzer, but the primer and adaptor dimers were mixed in the libraries of patients 1 and 9 (Fig. 1A). Before deep sequencing, we evaluated whether the HCV genome was included in the libraries, and the amplification plots for quantitative PCR showed that the HCV genome could be detected in the libraries from both patients 1 and 7 with the specific primers C112 and C113, derived from the NS4B region (Fig. 1B).

Distribution of free RNA in human serum. To characterize the metagenomics of HCV infection in humans, we analyzed

TABLE 2 Distribution of viral reads in human serum

Sample	No. (%) of reads		
	Patient 1 (treatment naïve)	Patient 7 (treatment experienced)	Patient 9 (healthy control)
Total reads	27,717,487 (100.00)	94,151,356 (100.00)	15,032,130 (100.00)
Adaptor and primer reads	6,502,508 (23.46)	28,605,006 (30.38)	5,713,994 (38.01)
Modified total reads	21,214,979 (76.54)	65,546,350 (69.62)	9,318,136 (61.99)
Reads of human origin	19,761,560 (71.30)	58,446,916 (62.08)	8,660,143 (57.61)
Unknown reads	1,453,419 (5.24)	7,099,434 (7.54)	657,993 (4.38)

the samples by single-end deep sequencing on three lanes for patient 7 and on two lanes for patient 1 and control patient 9, using an Illumina IIx genome analyzer. After trimming the reads to exclude ambiguous nucleotides, primers, or adaptor sequences, 96,079,465 high-quality 76-bp reads were subjected to analysis. From the initial set of reads, a total of 86,868,619 reads were able to be aligned to human genomic DNA.

We then mapped the remaining 9,210,846 reads, including 1,453,419 reads for patient 1, 7,099,434 reads for patient 7, and 657,993 reads for patient 9 (Table 2).

Mapping of the HCV genome sequence. The reads were aligned to 970 HCV genome sequences by using BWA, allowing mismatches within 5 to 10 nucleotide bases. Accordingly, MD5-1 (GenBank accession no. AF165053) was expected to be the closest HCV strain to that in patient 1, and MD2-2 (GenBank accession no. AF165048) was expected to be the closest to that in patient 7. The reads obtained from healthy subject 9 were not aligned to MD5-1 or MD2-2, allowing mismatches within 10 nucleotide bases (see the supplemental material). Whereas some strains, for example, HC-J4, HCV-KT9, and HC-J6, could be mapped to the reads from healthy subject 9, all of the reads were aligned at the 3′-UTR of the U-rich region, and we could not evaluate whether they were of HCV origin. Therefore, we constituted the HCV genome sequences of patients 1 and 7 without the 3′-UTR. In this alignment, the duplicate reads were completely excluded. For patient 1, 6,303 reads were mapped on MD5-1, allowing for 10 mismatched nucleotide bases. The coverage was 99.4%, and the average depth was 51.1× (Fig. 2). For patient 7, 8,583 reads could be identified with MD2-2. The coverage was 99.8%, and the average sequencing depth was 69.5× (Fig. 2).

Notably, the genome sequence could not be obtained for only 8 nt in the 5′-UTR and 52 nt in the core region for patient 1 and for 18 nt in the E2 region for patient 7.

Amino acid substitutions in the core region and the NS5A ISDR. To identify potential mutations at key sites in the genome that mediate the effect of IFN-based therapy, we compared the HCV genome obtained from patient 7 with HCV-J, which is known as the prototypical HCV 1b strain and whose complete genomic sequence has been determined (20). A previous study reported that there were substitutions of aa 70 and/or 91 in the core region and that the number of substitutions within three bases in the region of aa 2209 to 2248 (NS5A ISDR) might be associated with resistance to IFN-based therapy (1, 2, 9, 10). Position 70 in the core region showed arginine, with methionine at aa 91, by Sanger sequencing. In deep sequencing, major variants showed the same amino acid sequence, but minor variants were detectable in 18% (6/34 sequences) of sequences, with replacement of methionine by leucine at aa 91 (Fig. 3A). In the NS5A ISDR, no substitution was indicated for major variants, the same as in direct sequencing by Sanger sequencing, but 16% (14/89 sequences) of sequences showed minor variant replacements of aspartic acid by valine at aa 2220 (Fig. 3B). We validated that more than 10% of the detected variants were effective. For patient 1, core aa 70 (arginine), core aa 91 (leucine), and the number of

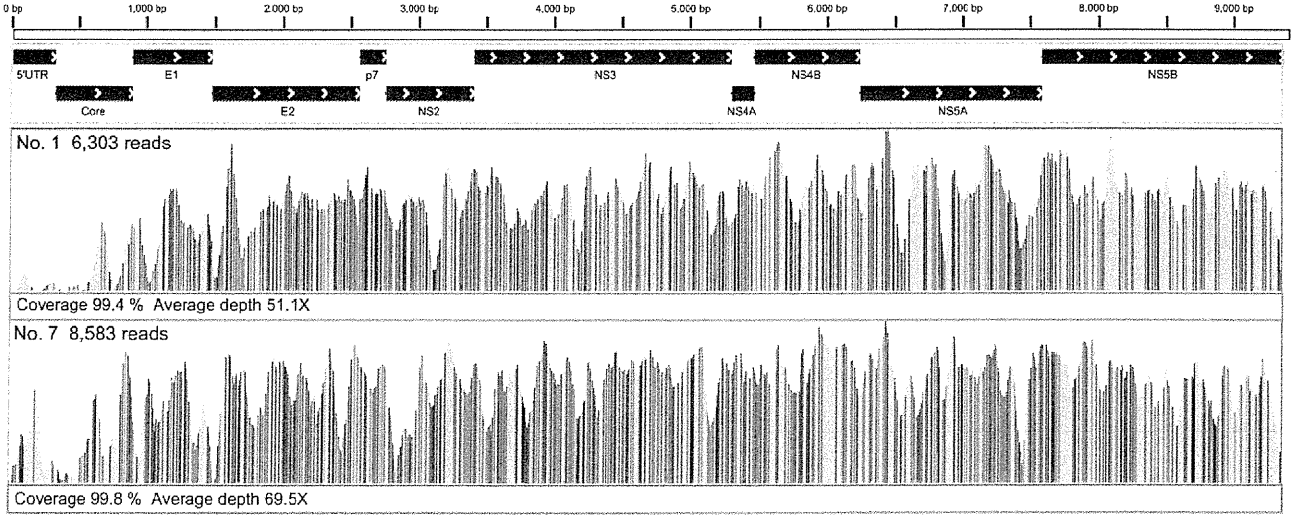

FIG 2 Mapping to the HCV reference genome. For patient 1, 6,303 reads were mapped to MD5-1. The coverage was 99.4%, and the average depth was 51.1×. For patient 7, 8,583 reads were aligned to MD2-2. The coverage was 99.8%, and the average depth was 69.5%.

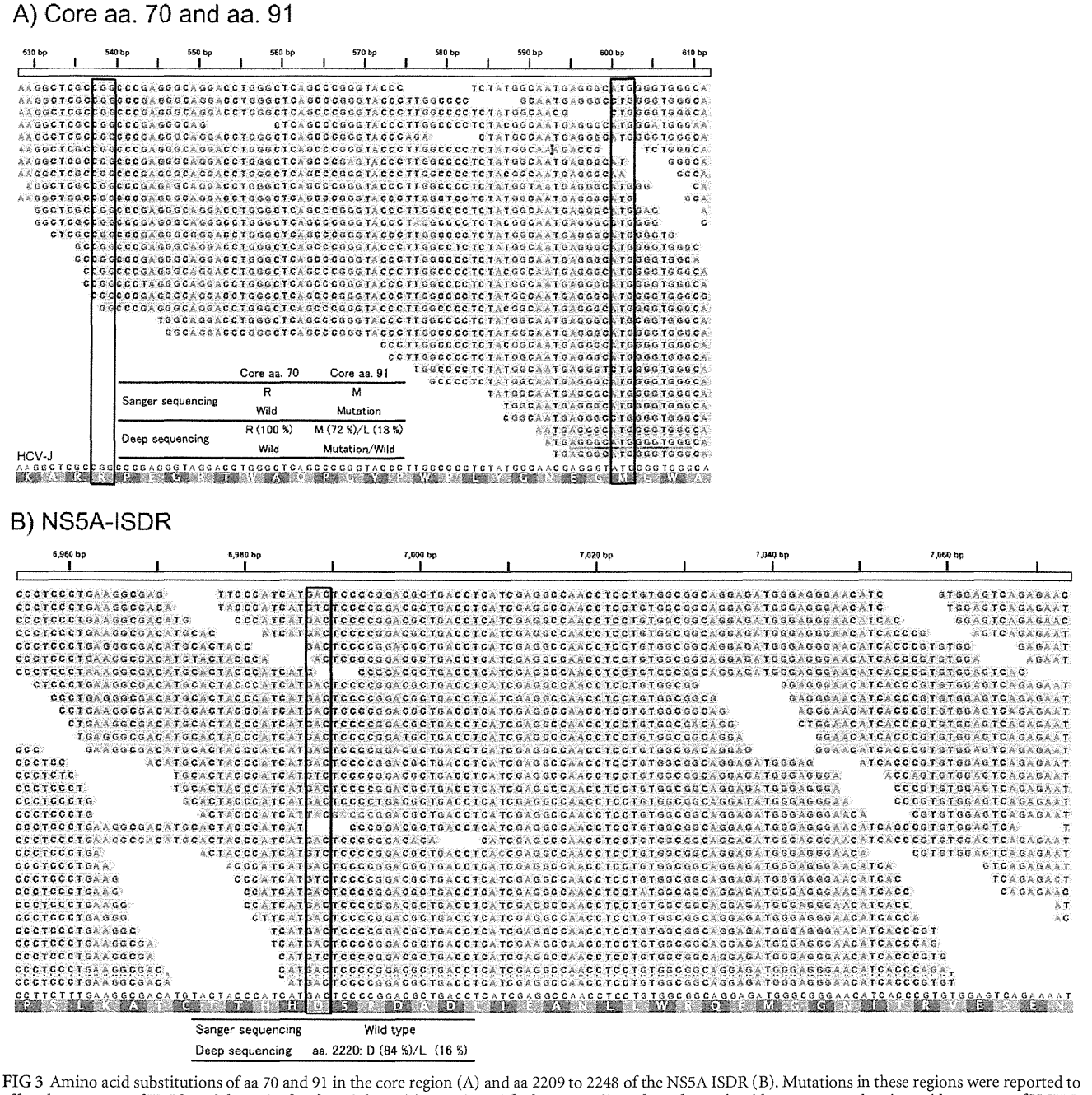

FIG 3 Amino acid substitutions of aa 70 and 91 in the core region (A) and aa 2209 to 2248 of the NS5A ISDR (B). Mutations in these regions were reported to affect the outcome of IFN-based therapies for chronic hepatitis C patients. The lower two lines show the nucleotide sequence and amino acid sequence of HCV-J. Amino acid abbreviations: F, phenylalanine; S, serine; Y, tyrosine; C, cysteine; W, tryptophan; L, leucine; P, proline; H, histidine; Q, glutamine; R, arginine; I, isoleucine; M, methionine; T, threonine; N, asparagine; K, lysine; V, valine; A, alanine; D, aspartic acid; E, glutamic acid; G, glycine.

NS5A ISDR mutations (zero) were the same as those by Sanger sequencing.

Amino acid substitutions in NS3 and NS5B. The recent development of DAA molecules, such as protease inhibitors and polymerase inhibitors, has raised the concern that resistance may weaken the effects of DAA-based therapy (35). It is necessary to obtain the amino acid sequences of NS3 or NS5B variants bearing substitutions which alter the target of the drug. In NS3 in the virus from patient 7, 26 amino acids were changed in comparison with the prototype strain HCV-J. Eight amino acids showed mixed variants, with T72T/I (57 variants [75%]/21 variants [27%]), K213K/R (18 variants [26%]/52 variants [74%]), G237G/S (41 variants [46%]/49 variants [54%]), P264P/S/A (20 variants [42%]/19 variants [40%]/9 variants [19%]), S297S/A (63 variants [81%]/15 variants [19%]), A358A/T (20 variants [21%]/75 variants [79%]), S457S/C (56 variants [64%]/32 variants [36%]), and I615I/M (42 variants [46%]/49 variants [54%]) substitutions (Table 3). For NS5B, the full amino acid sequence was observed, and

TABLE 3 Amino acid substitutions compared with HCV-J in NS3 and NS5B from viruses of patients 1 and 7

Protein and patient	Nucleotide position	Amino acid position	Prototype amino acid	Nucleotide sequence[a]	Amino acid substitution[b]
NS3					
Patient 1	3426	7	S	gCC	A
	3447	14	L	(C/t/g)TT	L/F/V (67 [89]/6 [8]/2 [3])
	3495	30	D	GAg	E
	3513	36	L	gTt	V
	3588	61	S	(T/g)CG	S/A (48 [71]/20 [29])
	3591	62	K	AgG	R
	3618	71	I	gTC	V
	3645	80	Q	CtG	L
	3663	86	P	CaG	Q
	3747	114	V	aTc	I
	3801	132	I	gTC	V
	3855	150	V	GcT	A
	3915	170	I	gT(A/g)	V
	4149	248	I	gTC	V
	4152	249	E	GAc	D
	4191	262	G	aGC	S
	4194	263	G	Gct	A
	4218	271	C	gGC	G
	4302	299	T	tCC	S
	4392	329	I	gTC	V
	4479	358	A	aaC	N
	4551	382	T	tCg	S
	4554	382	G	GcC	A
	4563	386	L	gTC	V
	4659	418	F	TaT	Y
	4758	451	L	gTG	V
	4782	459	A	tCG	S
	4815	470	S	gGg	G
	4935	510	S	aCa	T
	5007	534	S	gGC	G
	5076	557	L	tTC	F
	5163	586	I	A(T/c)A	I/T (4 [12]/30 [88])
	5232	609	V	aTC	I
	5268	621	A	aCA	T
Patient 7	3495	30	D	GAg	E
	3513	36	L	gTt	V
	3531	42	S	aCT	T
	3549	48	V	aTC	I
	3621	72	T	A(C/t)C	T/I (57 [73]/21 [27])
	3663	86	P	CaG	Q
	3672	89	P	tCC	S
	3687	94	M	tTG	L
	3747	114	V	aTc	I
	3801	132	I	gTC	V
	3855	150	V	GcT	A
	3915	170	I	gTA	V
	4044	213	K	A(A/g)g	K/R (18 [26]/52 [74])
	4116	237	G	(G/a)G(C/t)	G/S (41 [46]/49 [54])
	4149	248	I	gTt	V
	4152	249	E	Gac	D
	4194	263	G	Gct	A
	4197	264	P	(C/t/g)CC	P/S/A (20 [42]/19 [40]/9 [19])
	4218	271	C	gGC	G
	4296	297	S	(T/g)CG	S/A (63 [81]/15 [19])
	4302	299	T	tCC	S
	4479	358	A	(G/a)CC	A/T (20 [21]/74 [79])
	4542	379	A	tCA	S
	4551	382	T	tCA	S
	4554	383	G	acC	T
	4563	386	L	aTC	I
	4659	418	F	TaT	Y
	4758	451	L	gTG	V
	4776	457	S	T(C/g)(G/t)	S/C (56 [64]/32 [36])
	4782	459	A	tCg/a	S
	4815	470	S	gcg	A
	5076	557	L	tTC	F
	5172	589	K	AgG	R
	5250	615	I	AT(A/g)	I/M (42 [46]/49 [54])
	5259	618	Y	TtC	F

(Continued on following page)

TABLE 3 (Continued)

Protein and patient	Nucleotide position	Amino acid position	Prototype amino acid	Nucleotide sequence[a]	Amino acid substitution[b]
NS5B					
Patient 1	7659	25	P	gCG	A
	7689	35	S	Aac	N
	7701	39	S	gCC	A
	7725	47	L	CaG	Q
	7827	81	R	Aaa	K
	7839	85	I	gTA	V
	7878	98	K	AgA	R
	7914	110	S	AaC	N
	7932	116	V	aTt	I
	7944	120	R	CaC	H
	7956	124	E	aAG	K
	7989	135	D	aAc	N
	8025	147	V	aTt	I
	8151	189	P	tCC	S
	8205	207	T	gCC	A
	8223	213	C	aaC	N
	8238	218	S	gCA	A
	8289	235	T	gtT	V
	8370	262	V	aTt	I
	8484	300	T	tCT	S
	8532	316	N	tgC	C
	8589	335	A	aaC	N
	8598	338	A	GtC	V
	8784	400	V	GcT	A
	8937	451	C	acT	T
	8976	464	E	cAg	Q
	9153	523	K	Aga	R
	9177	531	K	AgG	R
	9252	556	N	AgC	S
	9276	564	L	gTG	V
	9306	574	L	TgG	W
Patient 7	7599	5	T	tCA	S
	7689	35	S	Aa(c/t)	N
	7701	39	S	gCC	A
	7725	47	L	Caa	Q
	7827	81	R	Aaa	K
	7839	85	I	gTg	V
	7878	98	K	AgA	R
	7914	110	S	AaC	N
	7926	114	R	Aaa	K
	7956	124	E	aAG	K
	8151	189	P	tCC	S
	8205	207	T	gCC	A
	8223	213	C	acC	T
	8238	218	S	gCA	A
	8277	231	N	AgT	S
	8289	235	T	gtT	V
	8298	238	S	gCA	A
	8370	262	V	aTC	I
	8484	300	T	tCT	S
	8532	316	N	tgC	C
	8589	335	A	agC	S
	8784	400	V	GcT	A
	8937	451	C	acT	T
	8940	452	Y	cAC	H
	8946	454	I	gTT	V
	8976	464	E	cAA	Q
	9177	531	K	AgG	R
	9213	543	S	TtC	F
	9231	549	G	aaC	N
	9252	556	N	AgC	S
	9306	574	L	TgG	W

[a] Uppercase letters indicate prototype nucleotides, and lowercase letters indicate mutations.

[b] The numbers and percentages of amino acid bases are displayed in parentheses and brackets, respectively.

31 amino acids were altered in comparison with HCV-J. No mixed variants were seen (Table 3). With patient 1, full amino acid sequences were detected for NS3 and NS5B. Compared with HCV-J, 31 amino acids were altered in NS3, and 3 amino acids showed mixed variants, with L14L/F/V (67 variants [89%]/6 variants [8%]/2 variants [3%]), S61S/A (48 variants [71%]/20 variants [29%]), and I586I/T (4 variants [12%]/30 variants [88%]) substitutions (Table 3). In NS5B, 31 amino acids were converted (Table 3). Note that more than 10% of the minor variants were confirmed as effective.

DISCUSSION

In this study, we attempted to detect the HCV genome directly in human serum without using specific primers and succeeded in determining and certifying nearly the full genome sequence and a high genetic diversity by using deep Illumina sequencing. HCV has already been reported to be a highly variable virus with a quasispecies distribution, large viral populations, and very rapid turnover in individual patients (6, 26). Previous studies using metagenomic sequencing of other viruses from human clinical samples mostly employed pyrosequencing (11, 12, 23, 30, 46). The longer reads from pyrosequencing (250 to 450 bp) facilitate the assembly of individual reads into contigs, which facilitates the classification of the sequence data by homology-based BLAST alignment. In contrast to metagenomic analysis using pyrosequencing, Illumina short-read sequencing enables a greater depth (by an order of magnitude) that is reflected in a very low detection limit. A recent report revealed that viral transcripts could be found at frequencies of <1 in 1,000,000 (28). However, because of short reads, *de novo* assembly without any reference is difficult to conduct, so it is not suitable for discovering an unknown viral genome. However, it seems quite useful for resequencing or detection of variants of known viruses for which abundant nucleotide sequence data have already been reported.

We defined the Illumina 76-mer reads as being of HCV origin by relying on the 970 HCV genome sequences in this study. HCV shows considerable genetic diversity and has been classified into 11 genogroups or 6 groups by the core, E1, or NS5B region, with nucleotide divergence. Only about 75% similarity was shown in the variable region, even for the same group (38, 39, 44). The reads were aligned to each of the 970 HCV sequences, allowing mismatches within 10 nucleotide bases. Under these conditions, we could not map the reads of HCV isolates without the 3′-UTR region for patient 9, who had not been infected with HCV. This is because the 3′-UTR has a U-rich region, and it is impossible to decide the reads of HCV origin with specificity. Therefore, we aligned the reads to the full HCV sequence without the 3′-UTR for patients 1 and 7.

Many variants with different nucleotide bases, known as quasispecies, were detected in both patients 1 and 7. Taking a close look at the mixed variants with amino acid substitutions in NS3, patient 7 showed 8 variants, while there were only 3 variants in patient 1. Recent studies reported that HCV genomic sequences in treatment relapsers displayed significantly more mutations than those in nonresponders. HCV sequence analysis of a 4-year post-antiviral-therapy follow-up revealed that the vast majority of mutations selected during the therapy phase were maintained in the relapsers, while very few new mutations arose during the 4-year posttherapy span (5, 47). Based on the experiments mentioned above, treatment with IFN may lead to the emergence of mutations. Deep sequencing is considered a useful tool for detecting viral variants and determining the mutational rate without cloning.

Although there were only a few detected reads of HCV origin obtained from serum, metagenomic analysis could be conducted with the enormous data sets generated by deep sequencing. Consequently, almost the full genome sequence of HCV was demonstrated by using computational analysis of sequential alignments of individual reads, with average depths of 51.1× and 69.5×. However, the regions for which we could not obtain the sequence were 8 nt in the 5′-UTR and 52 nt in the core region for patient 1 and 18 nt in the E2 region for patient 7. Since the 5′-UTR forms on characteristic stem-loop structures, Sanger sequencing is generally difficult (31). Similarly, even deep Illumina sequencing appears to be difficult. Since the E2 region, known as a hypervariable region, is reported to have extreme sequence variability, it was predicted that there would be too many mismatches with the reference HCV genome and that the reads could not be mapped by this analysis. Analysis of this hypervariable region will require further work.

Comparing the qualities of the libraries from patients 1 and 7, that of patient 7 was well refined; hence, the quality of the library is important for gaining large amounts of expected reads. However, a lot of duplicate reads were found for patient 7, and in fact, to analyze the full sequence of HCV, it is considered sufficient to use two lanes for Illumina sequencing.

Amino acid substitutions of core aa 70 and 91 and within the NS5A ISDR, as well as genetic polymorphisms in the host IL28B gene, encoding IFN-λ-3 on chromosome 19, affect the outcome of interferon-based therapies for chronic hepatitis C patients (1, 2, 9, 10, 16, 40, 43). Even if only the amino acid substitution of a major variant were assumed, an accurate therapeutic effect would be impossible to predict. The proportion of minor variants may change the therapeutic effect, and variants cannot be detected only by direct sequencing using Sanger sequencing. In fact, patient 7 showed a methionine at aa 91 in the core region and no substitution in the NS5A ISDR by direct Sanger sequencing, but deep sequencing indicated minor variants (at aa 91 in the core region [18% of sequences] and in the NS5A ISDR [15% of sequences]).

Recently, DAA molecules have been developed for HCV therapies, and these drugs may lead to the selection of resistant viruses if administered alone. The first-generation NS3/4A inhibitors are telaprevir and boceprevir, and most of the reported clinical data on drug resistance were obtained from patients treated with telaprevir. As an illustration, based on *in vitro* studies, telaprevir resistance related to amino acid substitutions V36A/M/C, T54A/S, R155K/T/Q, A155V/T, and A156T has been reported (4, 22, 37). Substitutions that generated boceprevir resistance included those detected in a patient treated with telaprevir, plus V170A/T and V55A substitutions (13, 41). Of the nonnucleoside inhibitors of RdRp displaying inhibitory activities against the RdRp enzyme at NS5B, few have been reported in the *in vivo* resistance data (27). This is because studies of antiviral efficacy are generally limited to 3 to 5 days. Yet, for example, the S282T substitution has been reported to confer a loss of *in vitro* sensitivity to nucleoside/nucleotide analogue inhibitors (3). In the future, the triple combination of peg-IFN-α, RBV, and a protease inhibitor or several combina-

tions of DAAs will soon become the standard therapy for treatment-naïve and treatment-experienced patients with HCV genotype 1. In this study, though neither patient 1 nor patient 7 showed drug-resistant variants, it would be very important for the selection of therapy to identify resistant or minor variants prior to treatment. Additionally, when treatment has failed, it is necessary to consider viral factors as a cause.

In conclusion, deep sequencing technologies are a powerful tool for obtaining more profound insight into the dynamics of variants in the HCV quasispecies in human serum. Although the cost of deep sequencing is still much greater than the reagent costs for Sanger sequencing, it is still attractive in clinical medicine because deep sequencing is able to generate much more information on the viral genome sequences in internal organs. The cost will decrease in the future as the technology of deep sequencing develops. As DAA combination treatment of HCV infection is developed, obtaining sequence information on variants in individual cases by use of deep sequencing will be feasible for determining optimal antiviral treatment.

ACKNOWLEDGMENTS

We thank M. Tsuda, N. Koshita, and K. Kuroda for technical assistance. We also acknowledge the support of the Biomedical Research Core of the Tohoku University Graduate School of Medicine.

This study was supported in part by a Grant-in-Aid for Young Scientists (B) from the Ministry of Education, Culture, Sports, Science, and Technology of Japan (assignment no. 22790627) and by grants from the Ministry of Health, Labor, and Welfare of Japan.

REFERENCES

1. **Akuta N, et al.** 2007. Prediction of response to pegylated interferon and ribavirin in hepatitis C by polymorphisms in the viral core protein and very early dynamics of viremia. Intervirology **50**:361–368.
2. **Akuta N, et al.** 2005. Association of amino acid substitution pattern in core protein of hepatitis C virus genotype 1b high viral load and non-virological response to interferon-ribavirin combination therapy. Intervirology **48**:372–380.
3. **Ali S, et al.** 2008. Selected replicon variants with low-level in vitro resistance to the hepatitis C virus NS5B polymerase inhibitor PSI-6130 lack cross-resistance with R1479. Antimicrob. Agents Chemother. **52**:4356–4369.
4. **Barbotte L, et al.** 2010. Characterization of V36C, a novel amino acid substitution conferring hepatitis C virus (HCV) resistance to telaprevir, a potent peptidomimetic inhibitor of HCV protease. Antimicrob. Agents Chemother. **54**:2681–2683.
5. **Cannon NA, Donlin MJ, Fan X, Aurora R, Tavis JE.** 2008. Hepatitis C virus diversity and evolution in the full open-reading frame during antiviral therapy. PLoS One **3**:e2123.
6. **Choo QL, et al.** 1991. Genetic organization and diversity of the hepatitis C virus. Proc. Natl. Acad. Sci. U. S. A. **88**:2451–2455.
7. **Clavel F, Hance AJ.** 2004. HIV drug resistance. N. Engl. J. Med. **350**:1023–1035.
8. **Domingo E, et al.** 1985. The quasispecies (extremely heterogeneous) nature of viral RNA genome populations: biological relevance—a review. Gene **40**:1–8.
9. **Enomoto N, et al.** 1995. Comparison of full-length sequences of interferon-sensitive and resistant hepatitis C virus 1b. Sensitivity to interferon is conferred by amino acid substitutions in the NS5A region. J. Clin. Invest. **96**:224–230.
10. **Enomoto N, et al.** 1996. Mutations in the nonstructural protein 5A gene and response to interferon in patients with chronic hepatitis C virus 1b infection. N. Engl. J. Med. **334**:77–81.
11. **Feng H, Shuda M, Chang Y, Moore PS.** 2008. Clonal integration of a polyomavirus in human Merkel cell carcinoma. Science **319**:1096–1100.
12. **Finkbeiner SR, et al.** 2009. Identification of a novel astrovirus (astrovirus VA1) associated with an outbreak of acute gastroenteritis. J. Virol. **83**:10836–10839.
13. **Flint M, et al.** 2009. Selection and characterization of hepatitis C virus replicons dually resistant to the polymerase and protease inhibitors HCV-796 and boceprevir (SCH 503034). Antimicrob. Agents Chemother. **53**:401–411.
14. **Fried MW, et al.** 2002. Peginterferon alfa-2a plus ribavirin for chronic hepatitis C virus infection. N. Engl. J. Med. **347**:975–982.
15. **Gao M, et al.** 2010. Chemical genetics strategy identifies an HCV NS5A inhibitor with a potent clinical effect. Nature **465**:96–100.
16. **Ge D, et al.** 2009. Genetic variation in IL28B predicts hepatitis C treatment-induced viral clearance. Nature **461**:399–401.
17. **Honda M, Beard MR, Ping LH, Lemon SM.** 1999. A phylogenetically conserved stem-loop structure at the 5′ border of the internal ribosome entry site of hepatitis C virus is required for cap-independent viral translation. J. Virol. **73**:1165–1174.
18. **Honda M, et al.** 1996. Structural requirements for initiation of translation by internal ribosome entry within genome-length hepatitis C virus RNA. Virology **222**:31–42.
19. **Ina Y.** 1994. ODEN: a program package for molecular evolutionary analysis and database search of DNA and amino acid sequences. Comput. Appl. Biosci. **10**:11–12.
20. **Kato N, et al.** 1990. Molecular cloning of the human hepatitis C virus genome from Japanese patients with non-A, non-B hepatitis. Proc. Natl. Acad. Sci. U. S. A. **87**:9524–9528.
21. **Kieffer TL, et al.** 2007. Telaprevir and pegylated interferon-alpha-2a inhibit wild-type and resistant genotype 1 hepatitis C virus replication in patients. Hepatology **46**:631–639.
22. **Kwong AD, McNair L, Jacobson I, George S.** 2008. Recent progress in the development of selected hepatitis C virus NS3.4A protease and NS5B polymerase inhibitors. Curr. Opin. Pharmacol. **8**:522–531.
23. **Lataillade M, et al.** 2010. Prevalence and clinical significance of HIV drug resistance mutations by ultra-deep sequencing in antiretroviral-naive subjects in the CASTLE study. PLoS One **5**:e10952.
24. **Li H, et al.** 2009. The sequence alignment/map format and SAMtools. Bioinformatics **15**:2078–2079.
25. **Manns MP, et al.** 2001. Peginterferon alfa-2b plus ribavirin compared with interferon alfa-2b plus ribavirin for initial treatment of chronic hepatitis C: a randomised trial. Lancet **358**:958–965.
26. **Martell M, et al.** 1992. Hepatitis C virus (HCV) circulates as a population of different but closely related genomes: quasispecies nature of HCV genome distribution. J. Virol. **66**:3225–3229.
27. **McCown MF, et al.** 2008. The hepatitis C virus replicon presents a higher barrier to resistance to nucleoside analogs than to nonnucleoside polymerase or protease inhibitors. Antimicrob. Agents Chemother. **52**:1604–1612.
28. **Moore RA, et al.** 2011. The sensitivity of massively parallel sequencing for detecting candidate infectious agents associated with human tissue. PLoS One **6**:e19838.
29. **Moradpour D, Penin F, Rice CM.** 2007. Replication of hepatitis C virus. Nat. Rev. Microbiol. **5**:453–463.
30. **Nakamura S, et al.** 2009. Direct metagenomic detection of viral pathogens in nasal and fecal specimens using an unbiased high-throughput sequencing approach. PLoS One **4**:e4219.
31. **Ninomiya M, Takahashi M, Shimosegawa T, Okamoto H.** 2007. Analysis of the entire genomes of fifteen torque teno midi virus variants classifiable into a third group of genus Anellovirus. Arch. Virol. **152**:1961–1975.
32. **Okamoto H, et al.** 1992. Genetic drift of hepatitis C virus during an 8.2-year infection in a chimpanzee: variability and stability. Virology **190**:894–899.
33. **Okamoto H, et al.** 1992. Full-length sequence of a hepatitis C virus genome having poor homology to reported isolates: comparative study of four distinct genotypes. Virology **188**:331–341.
34. **Okamoto H, et al.** 1993. Characterization of the genomic sequence of type V (or 3a) hepatitis C virus isolates and PCR primers for specific detection. J. Gen. Virol. **74**:2385–2390.
35. **Pawlotsky JM.** 2011. Treatment failure and resistance with direct-acting antiviral drugs against hepatitis C virus. Hepatology **53**:1742–1751.
36. **Robinson JT, et al.** 2011. Integrative genomics viewer. Nat. Biotechnol. **29**:24–26.
37. **Sarrazin C, et al.** 2007. Dynamic hepatitis C virus genotypic and phenotypic changes in patients treated with the protease inhibitor telaprevir. Gastroenterology **132**:1767–1777.
38. **Simmonds P, et al.** 1994. Identification of genotypes of hepatitis C virus

by sequence comparisons in the core, E1 and NS-5 regions. J. Gen. Virol. 75:1053–1061.
39. **Smith DB, et al.** 1997. The origin of hepatitis C virus genotypes. J. Gen. Virol. 78:321–328.
40. **Suppiah V, et al.** 2009. IL28B is associated with response to chronic hepatitis C interferon-α and ribavirin therapy. Nat. Genet. 41:1100–1104.
41. **Susser S, et al.** 2009. Characterization of resistance to the protease inhibitor boceprevir in hepatitis C virus-infected patients. Hepatology 50: 1709–1718.
42. **Szpara ML, Parsons L, Enquist LW.** 2010. Sequence variability in clinical and laboratory isolates of herpes simplex virus 1 reveals new mutations. J. Virol. 84:5303–5313.
43. **Tanaka Y, et al.** 2009. Genome-wide association of IL28B with response to pegylated interferon-α and ribavirin therapy for chronic hepatitis C. Nat. Genet. 41:1105–1109.
44. **Tokita H, et al.** 1996. Hepatitis C virus variants from Jakarta, Indonesia classifiable into novel genotypes in the second (2e and 2f), tenth (10a) and eleventh (11a) genetic groups. J. Gen. Virol. 77:293–301.
45. **Verbinnen T, et al.** 2010. Tracking the evolution of multiple in vitro hepatitis C virus replicon variants under protease inhibitor selection pressure by 454 deep sequencing. J. Virol. 84:11124–11133.
46. **Victoria JG, et al.** 2009. Metagenomic analyses of viruses in stool samples from children with acute flaccid paralysis. J. Virol. 83:4642–4651.
47. **Xiang X, et al.** 2011. Viral sequence evolution in Chinese genotype 1b chronic hepatitis C patients experiencing unsuccessful interferon treatment. Infect. Genet. Evol. 11:382–390.

Am J Physiol Gastrointest Liver Physiol 301: G981–G991, 2011.
First published September 8, 2011; doi:10.1152/ajpgi.00061.2011.

Castration inhibits biliary proliferation induced by bile duct obstruction: novel role for the autocrine trophic effect of testosterone

Fuquan Yang,[1,6]* Sally Priester,[1,3]* Paolo Onori,[7] Julie Venter,[1] Anastasia Renzi,[1,10] Antonio Franchitto,[10,11] Md Kamruzzaman Munshi,[1,11] Candace Wise,[1] David E. Dostal,[2,5] Marco Marzioni,[8] Stefania Saccomanno,[8] Yoshiyuki Ueno,[9] Eugenio Gaudio,[10] and Shannon Glaser[1,4,5]

Department of Medicine, Division of [1]Gastroenterology and [2]Molecular Cardiology, Scott & White and Texas A&M Health Science Center, College of Medicine, [3]Research & Education, Scott & White, [4]Scott & White Digestive Disease Research Center, and [5]Central Texas Veterans Health Care System, Temple, Texas; [6]Department of Hepatobiliary Surgery, Shengjing Hospital, China Medical University, Shenyang, Liaoning Province, China; [7]Experimental Medicine, University of L'Aquila, L'Aquila; [10]Department of Anatomical, Histological, Forensic Medicine and Orthopedics Sciences, University of Rome "La Sapienza", Rome; Fondazione Eleonora Lorillard Spencer-Cenci, Rome; [8]Department of Gastroenterology, Università Politecnica delle Marche, Ancona, Italy, [9]Division of Gastroenterology, Tohoku Graduate University School of Medicine, Sendai, Japan; and [11]Institute of Food and Radiation Safety, Dhaka, Bangladesh

Submitted 15 February 2011; accepted in final form 29 August 2011

Yang F, Priester S, Onori P, Venter J, Renzi A, Franchitto A, Munshi MK, Wise C, Dostal DE, Marzioni M, Saccomanno S, Ueno Y, Gaudio E, Glaser S. Castration inhibits biliary proliferation induced by bile duct obstruction: novel role for the autocrine trophic effect of testosterone. *Am J Physiol Gastrointest Liver Physiol* 301: G981–G991, 2011. First published September 8, 2011; doi:10.1152/ajpgi.00061.2011.—Increased cholangiocyte growth is critical for the maintenance of biliary mass during liver injury by bile duct ligation (BDL). Circulating levels of testosterone decline following castration and during cholestasis. Cholangiocytes secrete sex hormones sustaining cholangiocyte growth by autocrine mechanisms. We tested the hypothesis that testosterone is an autocrine trophic factor stimulating biliary growth. The expression of androgen receptor (AR) was determined in liver sections, male cholangiocytes, and cholangiocyte cultures [normal rat intrahepatic cholangiocyte cultures (NRICC)]. Normal or BDL (immediately after surgery) rats were treated with testosterone or antitestosterone antibody or underwent surgical castration (followed by administration of testosterone) for 1 wk. We evaluated testosterone serum levels; intrahepatic bile duct mass (IBDM) in liver sections of female and male rats following the administration of testosterone; and secretin-stimulated cAMP levels and bile secretion. We evaluated the expression of 17β-hydroxysteroid dehydrogenase 3 (17β-HSD3, the enzyme regulating testosterone synthesis) in cholangiocytes. We evaluated the effect of testosterone on the proliferation of NRICC in the absence/presence of flutamide (AR antagonist) and antitestosterone antibody and the expression of 17β-HSD3. Proliferation of NRICC was evaluated following stable knock down of 17β-HSD3. We found that cholangiocytes and NRICC expressed AR. Testosterone serum levels decreased in castrated rats (prevented by the administration of testosterone) and rats receiving antitestosterone antibody. Castration decreased IBDM and secretin-stimulated cAMP levels and ductal secretion of BDL rats. Testosterone increased 17β-HSD3 expression and proliferation in NRICC that was blocked by flutamide and antitestosterone antibody. Knock down of 17β-HSD3 blocks the proliferation of NRICC. Drug targeting of 17β-HSD3 may be important for managing cholangiopathies.

biliary epithelium; biliary secretion; 17β-hydroxysteroid dehydrogenase 3; secretin; sex hormones

IN ADDITION TO PLAYING A KEY role in the ductal secretion of water and bicarbonate (mainly regulated by secretin) (3, 30), cholangiocytes are the target cells in a number of chronic cholestatic liver diseases (termed cholangiopathies), including primary sclerosing cholangitis and primary biliary cirrhosis (PBC) (5, 8). During the progression of cholangiopathies, the balance between the proliferation/loss of cholangiocytes is critical for the maintenance of biliary secretory function and intrahepatic bile ductal mass (5, 8, 34, 36). Cholangiocytes respond to cholestasis and liver injury with changes in proliferation and ductal bile secretion (2, 3, 18, 22). In response to bile duct ligation (BDL), there is enhanced biliary hyperplasia and secretin-stimulated choleresis (a functional marker of cholangiocyte growth) (2, 3, 18, 22), whereas, following the administration of hepatotoxins (e.g., carbon tetrachloride), there is loss of cholangiocyte mass and secretory function (36). Indeed, proliferating cholangiocytes serve as neuroendocrine cells secreting and responding to a number of hormones and neuropeptides contributing to the autocrine and paracrine pathways that modulate the homeostasis of the biliary epithelium (8, 16, 18, 19, 22, 23, 39).

Cholangiocyte growth/apoptosis is regulated by a number of factors, including gastrointestinal hormones, the second messenger system, cAMP, and sex hormones, including estrogens, prolactin, follicle-stimulating hormone, and progesterone (7, 8, 17, 23, 39, 49). Regarding sex hormones, estrogens have been shown to sustain cholangiocyte proliferation and reduce cholangiocyte apoptosis (6, 7). Prolactin is expressed and secreted by cholangiocytes and stimulates the growth of cholangiocytes by an autocrine mechanism (49). Progesterone enhances the proliferative activity of female and male cholangiocytes via autocrine mechanisms, since cholangiocytes possess the enzymatic pathway for steroidogenesis (23). Follicle-stimulating hormone increases cholangiocyte proliferation by an autocrine mechanism via cAMP-dependent phosphorylation of ERK1/2 and Elk-1 (39).

Testosterone is an anabolic steroid that is primarily secreted in the testes of males and the ovaries of females, although small amounts are also secreted by the adrenal glands. Testosterone is thought to predominantly mediate its biological effects through binding to the androgen receptor (AR) (43). Similar to other members of the nuclear receptor superfamily, ARs function as a ligand-inducible transcription factor. ARs are expressed in the liver by hepatocellular carcinoma, hepa-

* F. Yang and S. Priester contributed equally to this work.

Address for reprint requests and other correspondence: S. S. Glaser, Dept. of Medicine, Texas A&M Health Science Center, Central Texas Veterans Health Care System, VA Bldg. 205, 1901 South 1st St., Temple, TX, 76504 (e-mail: sglaser@medicine.tamhsc.edu).

tocytes in areas of ductular metaplasia, and in a number of metastatic adenocarcinomas, including bile duct cholangiocarcinoma (26, 44, 47). However, no information exists regarding the expression and role of testosterone and its receptors in the regulation of cholangiocyte growth and ductal secretory activity in cholestasis. The rate-limiting step in the synthesis of testosterone from androstenedione (a product of dehydroepiandrosterone and progesterone, both of which are products of pregnenolone and cholesterol) depends on the enzyme 17β-hydroxysteroid dehydrogenase 3 (17β-HSD3) (20). On the basis of these findings, we performed experiments aimed to demonstrate that: *1*) reduction of testosterone serum levels decreases cholangiocyte proliferation; *2*) testosterone administration stimulates biliary growth and prevents the decrease in biliary hyperplasia induced by castration; *3*) cholangiocytes express 17β-HSD3 and secrete testosterone regulating biliary by an autocrine mechanism; and *4*) silencing of 17β-HSD3 (the enzyme regulating testosterone synthesis) (20) decreases biliary proliferation in vitro. The data suggest an autocrine compensatory role of testosterone in sustaining cholangiocyte proliferation in cholestasis, a pathological condition characterized by testicular atrophy and lowered serum testosterone levels (14, 33, 54, 57).

MATERIALS AND METHODS

Materials. Reagents were purchased from Sigma Chemical (St. Louis, MO) unless otherwise stated. The monoclonal mouse antibody (clone PC-10) reacting with proliferating cellular nuclear antigen (PCNA) and the goat polyclonal antibody (antibody raised against a peptide mapping within an internal region of AR of human origin) reacting with both subtypes of AR were purchased from Santa Cruz Biotechnology (Santa Cruz, CA). The AR antibody (G-13) is recommended for the detection of AR of mouse, rat, and human origin. The substrate for γ-glutamyltranspeptidase (γ-GT), N-(γ-L-glutamyl)-4-methoxy-2-naphthylamide, was purchased from Polysciences (Warrington, PA). The enzyme-linked immunosorbebt assay (ELISA) kit used for measuring testosterone levels in serum and supernatant of primary cultures (after 6 h of incubation at 37°C) of isolated cholangiocytes from the selected groups of rats and primary cultures of rat intrahepatic cholangiocyte cultures [normal rat intrahepatic cholangiocyte cultures (NRICC)] from normal male rats (4) was purchased from Cayman Chemical (Ann Arbor, MI). The RIA kit (^{125}I-cAMP Biotrak Assay System, RPA509) for the determination of intracellular cAMP levels in purified cholangiocytes was purchased from GE Healthcare (Piscataway, NJ).

Animals. Female and male 344 Fischer rats (150–175 g) were purchased from Charles River (Wilmington, MA) and maintained in a temperature-controlled environment (20–22°C) with 12:12-h light-dark cycles. Animals were fed ad libitum standard chow and had free access to drinking water. The studies were performed in: *1*) normal and BDL female and male rats treated with sesame oil (vehicle) or testosterone in sesame oil (2.0 mg/100 g body wt) (10); *2*) normal male rats with castration (bilateral orchiectomy) (40) or sham; and *3*) BDL (for collection of liver blocks and cell isolation) (3) male rats (immediately after surgery) (3) that underwent sham or castration (40) followed by daily intraperitoneal injections of sesame oil or testosterone in sesame oil (2.0 mg/100 g body wt) (10) for 7 days. In other experiments, we treated BDL (immediately after surgery) male rats with nonimmune serum or a polyclonal immune-neutralizing testosterone antibody (6.5 nmol/dose ip every day, a dose similar to that used by us for immunoneutralizing other sex hormones such as progesterone) (23) for 7 days before collecting serum and liver blocks for the determination of biliary growth and apoptosis. Immediately after bile duct incannulation (for bile collection) (3), male rats underwent sham for castration or castration (followed by the administration of sesame oil or testosterone in sesame oil, 2.0 mg/100 g body wt for 1 wk) (10) before evaluating the effect of intravenous infusion of secretin on bile and bicarbonate secretion (3). Because there was no difference in biliary growth (data not shown) between normal rats treated with sesame oil and sham rats for castration or BDL rats treated with sesame oil or nonimmune serum and BDL sham rats for castration, we used only normal and BDL rats as controls in our study. Seven days later, the animals were killed for the collection of serum, liver block, bile, and cholangiocytes. Before each procedure, animals were anesthetized with pentobarbital sodium (50 mg/kg body wt ip) according to the regulations of the panel on euthanasia of the American Veterinarian Medical Association and local authorities. All experiments were reviewed and approved by the Scott & White Hospital/Texas A&M Health Science Center Institutional Animal Care and Use Committee.

Purification of cholangiocytes and hepatocytes. Virtually pure cholangiocytes (~98% by γ-GT histochemistry) (46) were isolated by immunoaffinity separation (27) using a mouse monoclonal antibody (IgM, kindly provided by Dr. R. Faris, Brown University, Providence, RI) that recognizes an unidentified antigen expressed by all intrahepatic rat cholangiocytes (27). Cell viability (by trypan blue exclusion) was ~98%. Hepatocytes were isolated from normal and BDL male rats as described (27). Male NRICC, which display morphological, phenotypic, and functional phenotypes similar to that of freshly isolated cholangiocytes, were developed, characterized, and maintained in culture as described by us (4).

Expression of AR and 17β-HSD3. The presence of AR was evaluated by: *1*) immunofluorescence (16) in frozen liver sections (4–5 μm thick) and immunohistochemistry (39) in paraffin-embedded liver sections (4–5 μm thick) from normal and BDL male rats; and *2*) RT-PCR (1) and fluorescence-activated cell sorter (FACS) analysis (45) in cholangiocytes and hepatocytes from normal and BDL male rats. In NRICC, the expression of AR was also evaluated by RT-PCR and immunofluorescence (39). For all immunoreactions, negative controls (with normal serum from the same species substituted for the primary antibody) were included.

With regard to RT-PCR (performed using the GeneAmp RNA PCR kit from Perkin-Elmer, Branchburg, NJ), specific oligonucleotide primers were based on the sequence of the rat AR (11) (sense, 5′-CCCTGTGTGTGCAGCTAGAA-3′ and antisense, 5′-TAGACAGGATCTGCCCTGCT-3′), with an expected fragment length of 247 bp; we used RNA (1 μg) from rat testicles and yeast-transfer RNA as positive and negative controls, respectively. The comparability of the RNA used was assessed by RT-PCR for the housekeeping gene glyceraldehyde-3-phosphate dehydrogenase (GAPDH) (sense 5′-GTGACTTCAACAGCAACTCCCATTC-3′ and antisense 5′-GTTATGGGGTCTGGGATGGAATTGTG-3′), with an expected fragment length of 294 bp; primers were based on the rat GAPDH sequence (15); rat kidney and yeast transfer RNA were the positive and negative controls for the GAPDH gene, respectively. Standard RT-PCR conditions were used, consisting of 35 step cycles: 30 s at 94°C, 30 s at 60°C for AR and 52°C for GAPDH for 45 s at 72°C. FACS analysis for AR was performed in isolated cholangiocytes and hepatocytes from normal and BDL rats using a C6 flow cytometer and analyzed by CFlow Software (Accuri Cytometers, Ann Arbor, MI). At least 20,000 events in the light scatter (side scatter/forward scatter) were acquired. The expression of AR was identified and gated on fluorescence channel 1-A (FL1-A)/count plots. The relative quantity of AR (mean selected protein fluorescence) was expressed as mean FL1-A (samples) per mean FL-1A (secondary antibodies only). The standard errors were calculated as (CV FL1-A) × (mean FL1-A)/SQR(count 1), where CV is coefficient of variation and SQR is square root.

We evaluated the expression of 17β-HSD3 (37) by: *1*) immunofluorescence (16) in frozen liver sections (4–5 μm thick) and immunohistochemistry (39) in paraffin-embedded liver sections (4–5 μm thick) from normal and BDL male rats; *2*) real-time PCR (16) and

FACS analysis (45) (see above) in freshly isolated male cholangiocytes; and *3*) real-time PCR and immunofluorescence (16) in male NRICC. For all immunoreactions, negative controls (with normal serum from the same species substituted for the primary antibody) were included. Following immunofluorescence for AR and 17β-HSD3, images were visualized using an Olympus IX-71 confocal microscope. Light microscopy photographs of liver sections stained for AR and 17β-HSD3 were taken by Leica Microsystems DM 4500 B Light Microscopy (Weltzlar, Germany) with a Jenoptik Prog Res C10 Plus Videocam (Jena, Germany). The positivity of bile ducts for AR and 17β-HSD3 was evaluated as described by us (25). When 0–5% of bile ducts were positive for AR and 17β-HSD3, we assigned a negative score; a ± score was assigned when 6–10% of bile ducts were positive; a + score was assigned when 11–30% of bile ducts were positive; a ++ score was assigned with 31–60% of bile ducts positive; and a +++ score was assigned when >61% of bile ducts were positive. Two pathologists performed the evaluations in a blinded manner.

For real-time PCR, total RNA was extracted from cholangiocytes by the RNeasy Mini Kit (Qiagen, Valencia, CA) and reverse transcribed using the Reaction Ready First-Strand cDNA synthesis kit (SuperArray, Frederick, MD). These reactions were used as templates for the PCR assays using a SYBR Green PCR master mix and specific primers designed against the rat 17β-HSD3 NM_054007 (51) and GAPDH, the housekeeping gene (SuperArray), in the real-time thermal cycler (ABI Prism 7900HT sequence detection system). A $\Delta\Delta C_T$ (delta delta of the threshold cycle) analysis was performed using normal cholangiocytes as the control sample. Data are expressed as fold change of relative mRNA levels ± SE (n = 6).

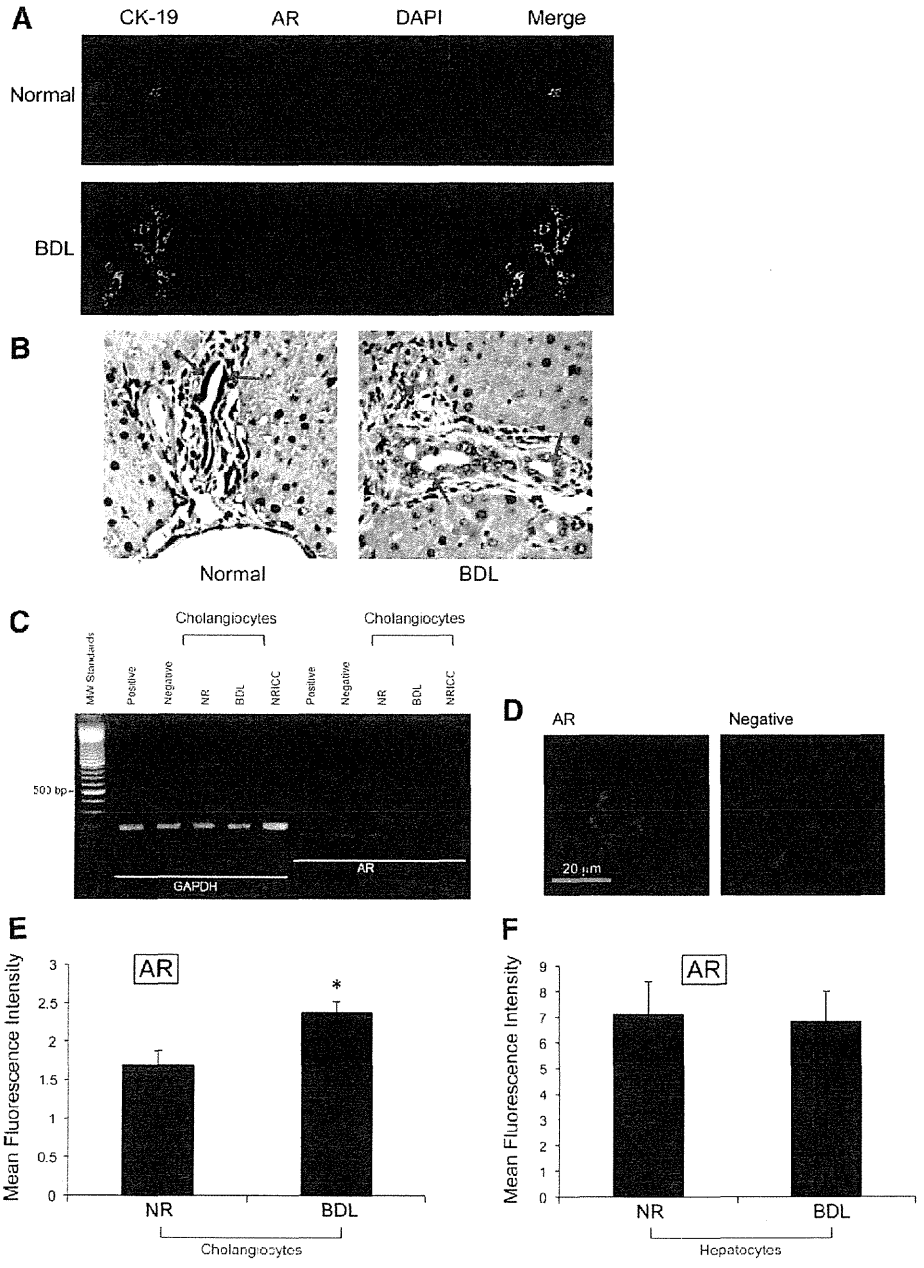

Fig. 1. *A*: image showing that intrahepatic bile ducts from normal and bile duct ligation (BDL) male rats express androgen receptor (AR) (red staining). Colocalization with CK-19 (green staining) of bile ducts expressing the AR (red staining) is also visible. Bar = 50 μm. *B*: by immunohistochemistry, normal cholangiocytes and hepatocytes express low levels of AR, expression that increased following BDL (*A* and *B*; see Table 1). Original magnification, ×40. *C*: by RT-PCR, the message for AR was expressed by freshly isolated cholangiocytes from normal (NR) and BDL rats and normal rat intrahepatic cholangiocyte cultures (NRICC); the housekeeping gene, glyceraldehyde-3-phosphate dehydrogenase (GAPDH), was expressed similarly by these cells. MW, mol wt. *D*: by immunofluorescence, NRICC also expressed the protein for AR. Bar = 20 μm. *E* and *F*: fluorescence-activated cell sorter (FACS) analysis shows the presence of the protein for AR in freshly isolated cholangiocytes and hepatocytes from normal and BDL male rats; the expression of AR seemed upregulated (*$P < 0.05$) in BDL cholangiocytes compared with normal cholangiocytes. Data are means ± SE of 3 determinations.

Table 1. *Semiquantitative analysis of AR expression in liver sections from normal and BDL male rats*

	Normal	BDL
Cholangiocytes	+	++
Hepatocytes	±	+

AR, androgen receptor; BDL, bile duct ligation. Grading scale: - = 0–5%; ± = 6–10%; + = 11–30%; ++ = 31–60%; +++ = >61%.

Evaluation of testosterone serum levels, cholangiocyte apoptosis, and intrahepatic bile duct mass in liver sections. Testosterone serum levels in female and male rats were measured by commercially available ELISA kits (Cayman Chemical). Cholangiocyte apoptosis was evaluated in paraffin-embedded liver sections (4–5 μm thick) by a quantitative terminal deoxynucleotidyl transferase biotin-dUTP nick end-labeling (TUNEL) kit (Apoptag; Chemicon International) (39). The percentage of TUNEL-positive cholangiocytes was counted in six nonoverlapping fields (magnification ×40) for each slide; the data are expressed as the percentage of TUNEL-positive cholangiocytes. The number of intrahepatic bile ducts in frozen liver sections (4–5 μm thick) was determined by the evaluation of intrahepatic bile duct mass (IBDM) by point-counting analysis (35, 56). IBDM was measured as the percentage area occupied by γ-GT-bile duct/total area × 100 (35, 56). Morphometric data were obtained in six different slides for each group; for each slide, we performed the counts in six nonoverlapping fields (n = 36). Following the selected staining, sections were counterstained with hematoxylin and eosin and analyzed for each group using a BX-51 light microscopy (Olympus, Tokyo, Japan).

Measurement of basal and secretin-stimulated cAMP levels and bile secretion. At the functional level, cholangiocyte proliferation was evaluated by measurement of basal and secretin-stimulated cAMP levels in purified cholangiocytes by RIA (17, 22, 32) and bile and bicarbonate secretion in bile fistula rats (3), two functional indexes of cholangiocyte proliferation (3, 17, 22). For the measurement of cAMP levels (17, 22), purified cholangiocytes (1×10^5) were incubated for 1 h at 37°C and incubated for 5 min at room temperature with 0.2% BSA (basal) or 100 nM secretin with 0.2% BSA (17, 22, 32). Following anesthesia with pentobarbital sodium, rats were surgically prepared for bile collection (3). When steady-state bile flow was reached [60–70 min from the infusion of Krebs-Ringer-Henseleit (KRH) solution], the animals were infused by a jugular vein with secretin (100 nM) for 30 min followed by a final infusion of KRH for 30 min. Bile was collected every 10 min in preweighed tubes that were used for determining bicarbonate concentration. Bicarbonate concentration (measured as total CO_2) in the selected bile sample was determined by an ABL 520 Blood Gas System (Radiometer Medical, Copenhagen, Denmark).

Effect of testosterone on the expression of 17β-HSD3 and proliferation of NRICC: Effect of pharmacological inhibition and molecular silencing of 17β-HSD3 on NRICC proliferation. To obtain a dose-response curve, NRICC were treated with vehicle (1% methanol, where testosterone is dissolved, basal value) or testosterone (10^{-5} to 10^{-11} M for 7 days in 1% methanol) before evaluating cell proliferation by MTS assays (16). We also evaluated the effects of testoster-

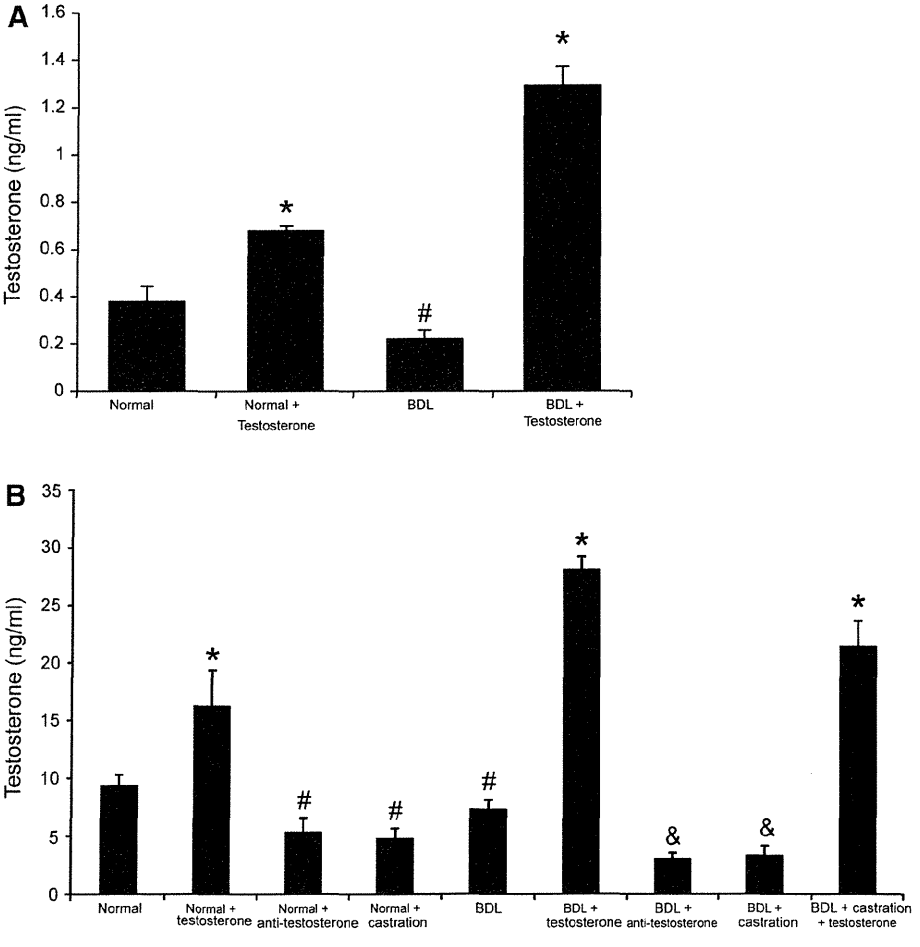

Fig. 2. Measurement of serum testosterone levels in the selected groups of animals. Testosterone serum levels were lower in female and male BDL rats compared with their corresponding normal rats. The administration of testosterone increased testosterone serum levels in normal and BDL female and male rats. Castration significantly decreased testosterone serum levels in normal and BDL rats. Administration of neutralizing antitestosterone antibody decreased testosterone serum levels in both normal and BDL rats compared with rats treated with nonimmune serum. The administration of testosterone to BDL castrated rats partly prevented castration-induced reduction of testosterone serum levels. Data are means ± SE of 12 cumulative determinations. *$P < 0.05$ compared with the corresponding values of normal rats. #$P < 0.05$ compared with the corresponding values of normal rats. &$P < 0.05$ compared with the corresponding values of BDL rats.

Table 2. *Measurement of IBDM in the experimental groups of animals*

Treatments	IBDM, %
Male	
Normal	0.26 ± 0.04
BDL	6.32 ± 0.67[a]
BDL testosterone	10.4 ± 0.80[b]
BDL + antitestosterone antibody	1.8 ± 0.14[b]
BDL + castration	0.32 ± 0.04[b]
BDL + castration + testosterone	5.48 ± 0.63
Female	
Normal	0.77 ± 0.14
BDL	4.01 ± 0.21[a]
BDL + testosterone	6.68 ± 0.89[b]

Values are means ± SE. IBDM, intrahepatic bile duct mass. $P < 0.05$ vs. IBDM of normal rats (a) and vs. IBDM of BDL rats (b).

one on the expression of message for 17β-HSD3 in NRICC. NRICC were stimulated with vehicle (1% methanol, where testosterone is dissolved, basal value) or testosterone (100 nM for 6, 24, 48, and 72 h in 1% methanol) before measuring 17β-HSD3 mRNA expression by real-time PCR (see above) (16).

In separate experiments, NRICC (after trypsinization) were seeded into 96-well plates (10,000/well) in a final volume of 200 μl of medium and allowed to adhere to the plate overnight. NRICC were incubated at 37°C with 0.2% BSA (basal), flutamide (a specific antagonist of AR, 10 μM) (28), or antitestosterone antibody (100 ng/ml with 0.2% BSA) for 48 h before evaluation of proliferation by MTS assays (16).

Furthermore, following stable transfection of 17β-HSD3 in NRICC (24), we measured the basal proliferative rates of the cells (after incubation for 24, 48, and 72 h at 37°C) by PCNA immunoblots and MTS assays (16). NRICC lacking 17β-HSD3 was established using SureSilencing shRNA (SuperArray) plasmid for rat 17β-HSD3 containing a marker for neomycin resistance for the selection of stably transfected cells, according to the instructions provided by the vendor as described by us (13). A total of four clones were assessed for the relative knock down of the 17β-HSD3 gene using real-time PCR (~80% knock down), and a single clone with the greatest degree of knock down was selected for subsequent experiments. In control vector- and 17β-HSD3-knocked cells, we also evaluated the amount of secreted testosterone (by ELISA kits) after incubation for 24 h at 37°C.

Statistical analysis. All data are expressed as means ± SE. Differences between groups were analyzed by the Student's unpaired *t*-test when two groups were analyzed and ANOVA when more than two groups were analyzed, followed by an appropriate post hoc test. A value of $P < 0.05$ was considered significant.

RESULTS

Expression of AR. By both immunofluorescence and immunohistochemistry in liver sections, we demonstrated that intrahepatic bile ducts from normal and BDL male rats express AR (Fig. 1, *A* and *B*). Colocalization of CK-19 (a cholangiocyte-specific marker) (18) with intrahepatic bile ducts expressing AR is visible in Fig. 1*A*. By immunohistochemistry, normal cholangiocytes and hepatocytes express low levels of AR, expression that increased following BDL (Fig. 1, *A* and *B*, and Table 1). By RT-PCR, the message for AR (247 bp) was expressed by freshly isolated cholangiocytes and hepatocytes from normal and BDL male rats and NRICC (Fig. 1*C*); the housekeeping gene, GAPDH mRNA (294 bp), was similarly expressed by these cells (Fig. 1*C*). By immunofluorescence, NRICC also expressed the protein for AR (Fig. 1*D*). We also demonstrated by FACS analysis the presence of AR in freshly isolated cholangiocytes and hepatocytes from normal and BDL male rats (Fig. 1, *E* and *F*); the expression of AR was upregulated in BDL compared with normal cholangiocytes (Fig. 1*E*).

Evaluation of testosterone serum levels, cholangiocyte apoptosis, and IBDM in liver sections. Parallel to previous studies (53, 54), testosterone serum levels were lower in female and male BDL rats compared with their corresponding normal rats (Fig. 2*A*). The serum levels of testosterone were lower in female rats compared with the corresponding values of male rats (Fig. 2*B*). The administration of testosterone increased testosterone serum levels in normal and BDL male rats (Fig. 2, *A* and *B*). Castration significantly decreased testosterone serum levels in normal and BDL male rats (Fig. 2*B*) (31). Similarly, administration of neutralizing antitestosterone antibody decreased testosterone serum levels in both normal and BDL male rats compared with rats treated with nonimmune serum (Fig. 2*B*). The administration of testosterone to BDL castrated rats partly prevented castration-induced reduction of testosterone serum levels (Fig. 2*B*). In female and male BDL rats, there

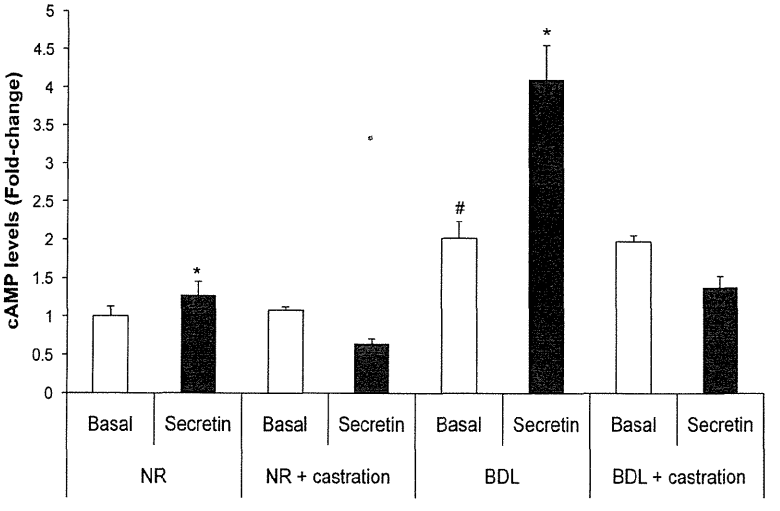

Fig. 3. Measurement of basal and secretin-stimulated cAMP levels in purified cholangiocytes. In normal and BDL rats (without castration), secretin increases cAMP levels of purified cholangiocytes. In purified cholangiocytes from normal and BDL castrated rats, there was ablation of the stimulatory effects of secretin on cAMP levels. *$P < 0.05$ vs. the corresponding basal cAMP levels. #$P < 0.05$ vs. basal cAMP levels of normal cholangiocytes. Data are means ± SE of 6 experiments.